Artificial Intelligence for Medical Imaging and Treatment Planning

Lei Xing, PhD, DABR, Jacob Haimson Professor

Departments of Radiation Oncology & Electrical Engineering (by courtesy), Human-Centered Artificial Intelligence (HAI)
Stanford University

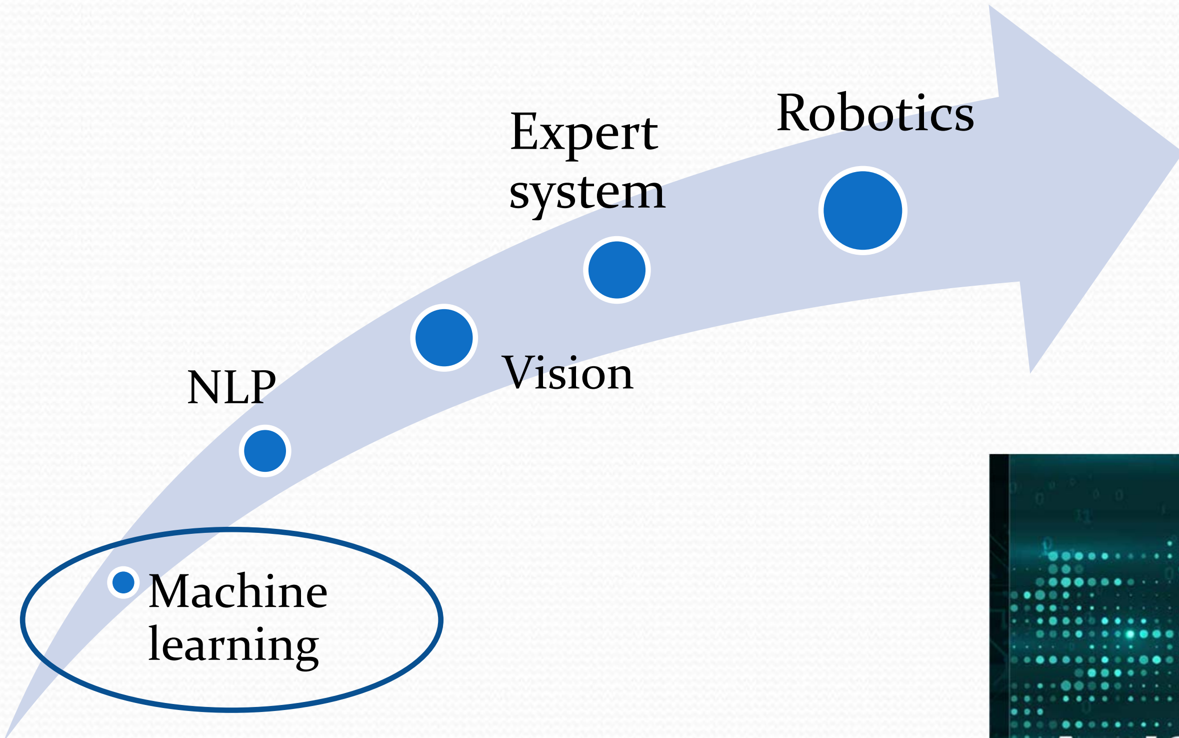
Robotics
Expert system
Vision
NLP
Machine learning


Artificial Intelligence

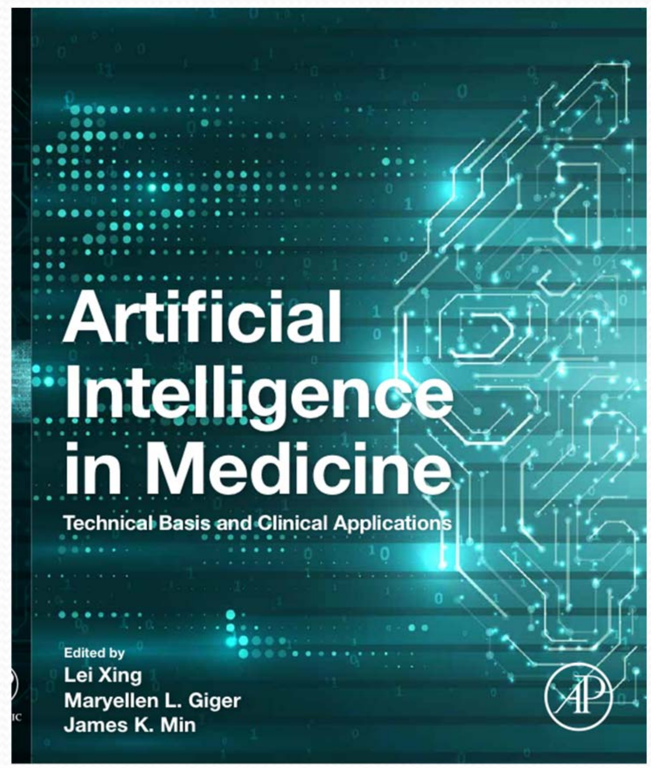
Artificial Intelligence in Medicine
Technical Basis and Clinical Applications
Edited by
Lei Xing
Maryellen L. Giger
James K. Min

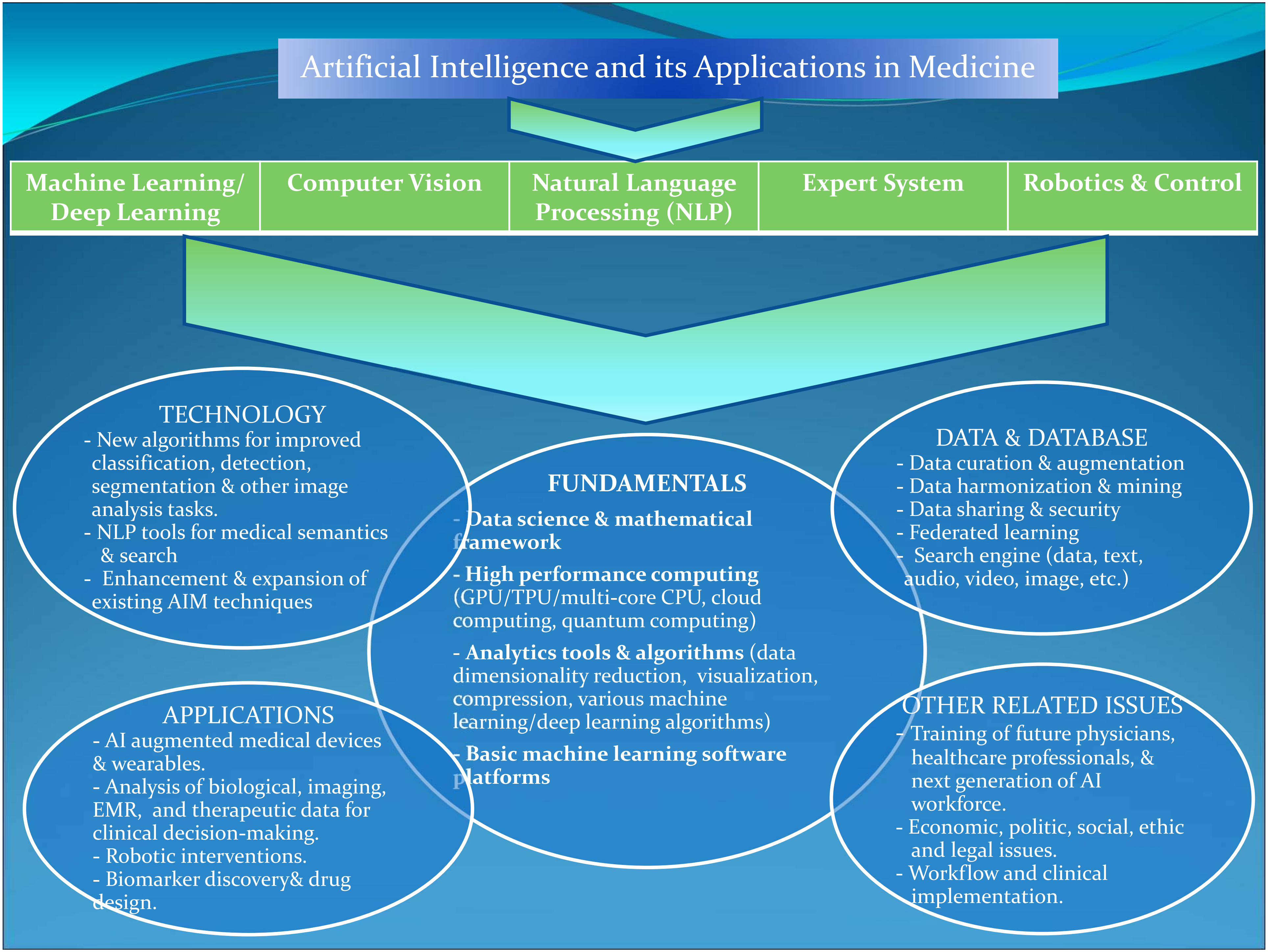
Artificial Intelligence and its Applications in Medicine
Machine Learning/ Deep Learning
Computer Vision
Natural Language Processing (NLP)
Expert System
Robotics & Control
TECHNOLOGY
- New algorithms for improved classification, detection, segmentation & other image analysis tasks.
- NLP tools for medical semantics & search
- Enhancement & expansion of existing AIM techniques
FUNDAMENTALS
- Data science & mathematical framework
- High performance computing (GPU/TPU/multi-core CPU, cloud computing, quantum computing)
- Analytics tools & algorithms (data dimensionality reduction, visualization, compression, various machine learning/deep learning algorithms)
- Basic machine learning software platforms
DATA & DATABASE
- Data curation & augmentation
- Data harmonization & mining
- Data sharing & security
- Federated learning
- Search engine (data, text, audio, video, image, etc.)
APPLICATIONS
- AI augmented medical devices & wearables.
- Analysis of biological, imaging, EMR, and therapeutic data for clinical decision-making.
- Robotic interventions.
- Biomarker discovery& drug design.
OTHER RELATED ISSUES
- Training of future physicians, healthcare professionals, & next generation of AI workforce.
- Economic, politic, social, ethic and legal issues.
- Workflow and clinical implementation.


Artificial Intelligence in Medicine
Technical Basis and Clinical Applications
Edited by
Lei Xing
Maryellen Giger
James K. Min

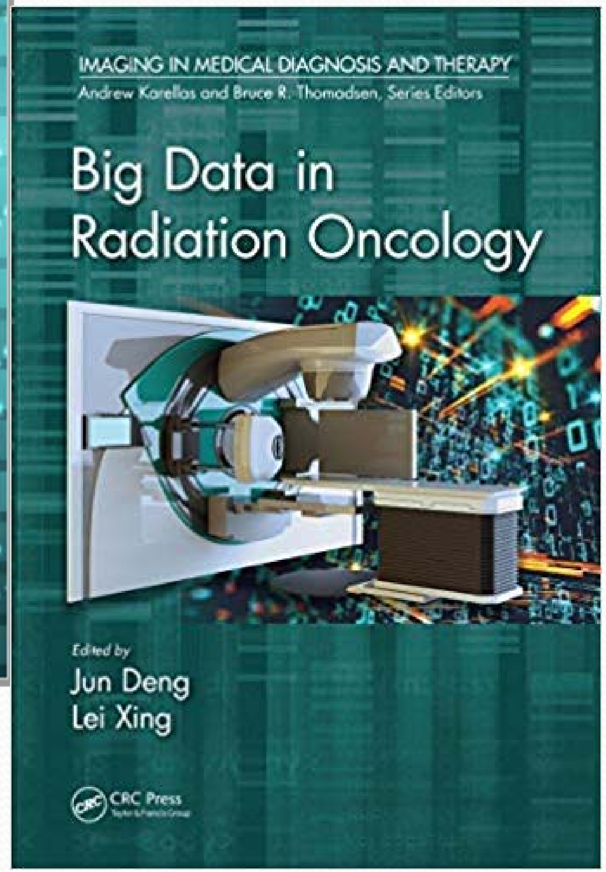
IMAGING IN MEDICAL DIAGNOSIS AND THERAPY
Andrew Karellas and Bruce R. Thomadsen, Series Editors
Big Data in Radiation Oncology
Edited by
Jun Deng
Lei Xing
CRC Press

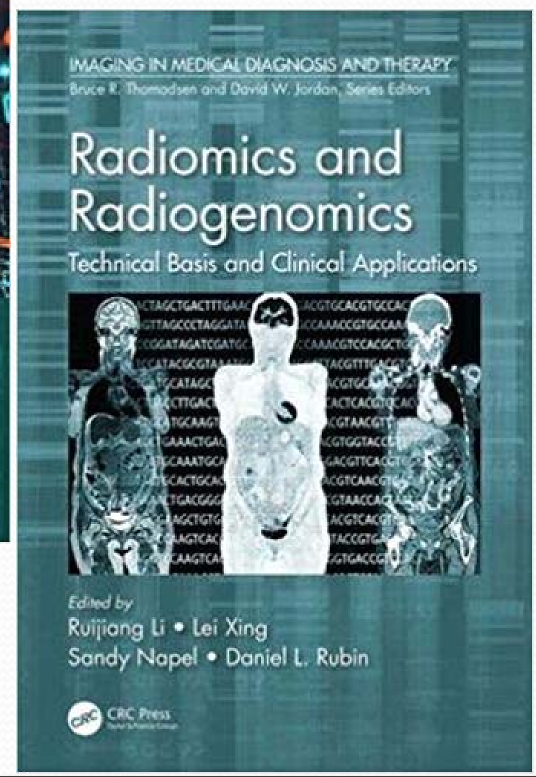
IMAGING IN MEDICAL DIAGNOSIS AND THERAPY
Bruce R. Thomadsen and David W. Jordan, Series Editors
Radiomics and Radiogenomics
Technical Basis and Clinical Applications
Edited by
Ruijiang Li • Lei Xing
Sandy Napel • Daniel L. Rubin
CRC Press

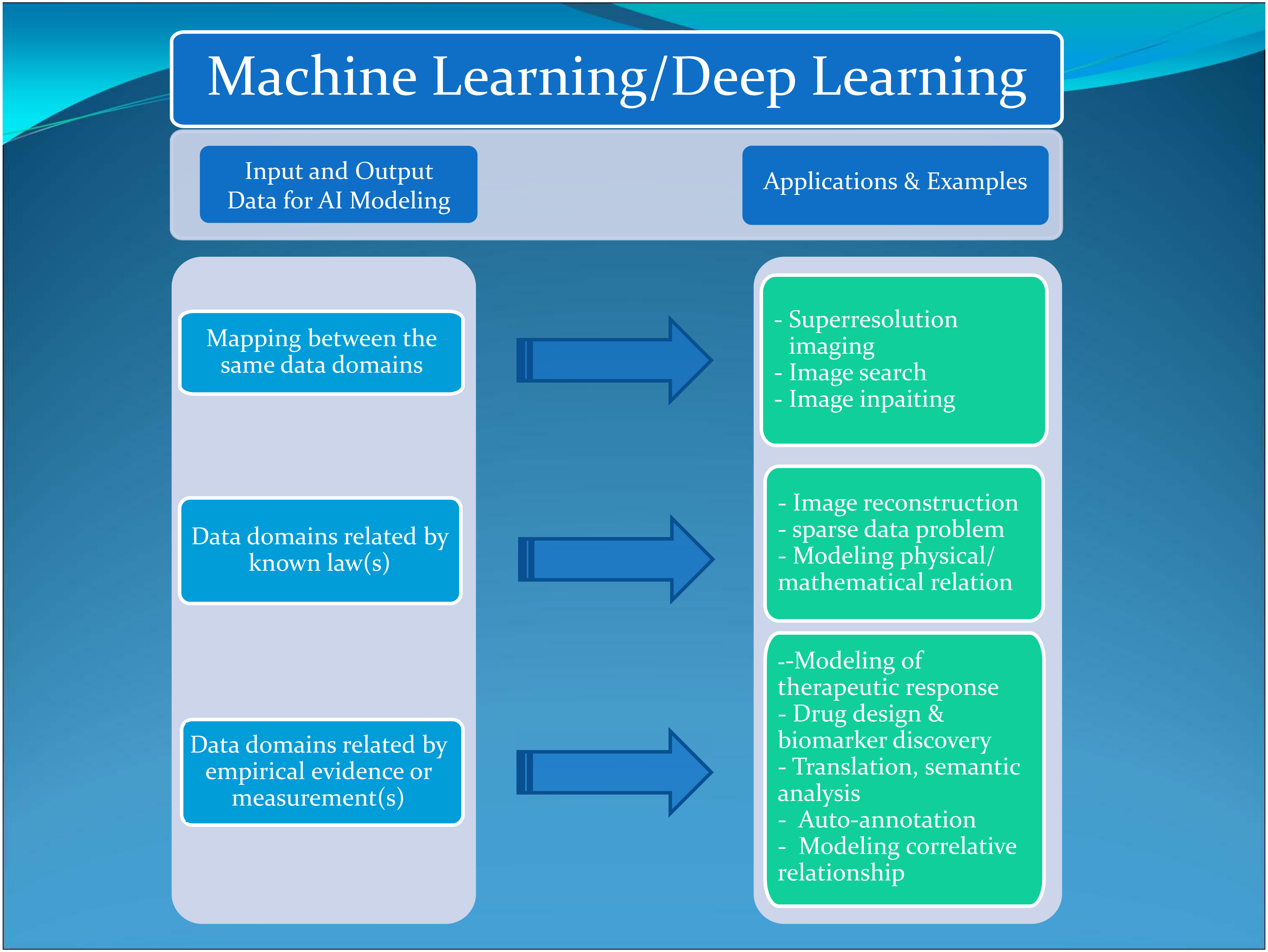
Machine Learning/Deep Learning
Input and Output Data for AI Modeling
Applications & Examples
Mapping between the same data domains
- Superresolution imaging
- Image search
- Image inpaiting
Data domains related by known law(s)
- Image reconstruction
- sparse data problem
- Modeling physical/ mathematical relation
Data domains related by empirical evidence or measurement(s)
--Modeling of therapeutic response
- Drug design & biomarker discovery
- Translation, semantic analysis
- Auto-annotation
- Modeling correlative relationship

Types of learning

- Supervised learning
- Unsupervised learning
- Reinforcement learning

Radiation oncology workflow

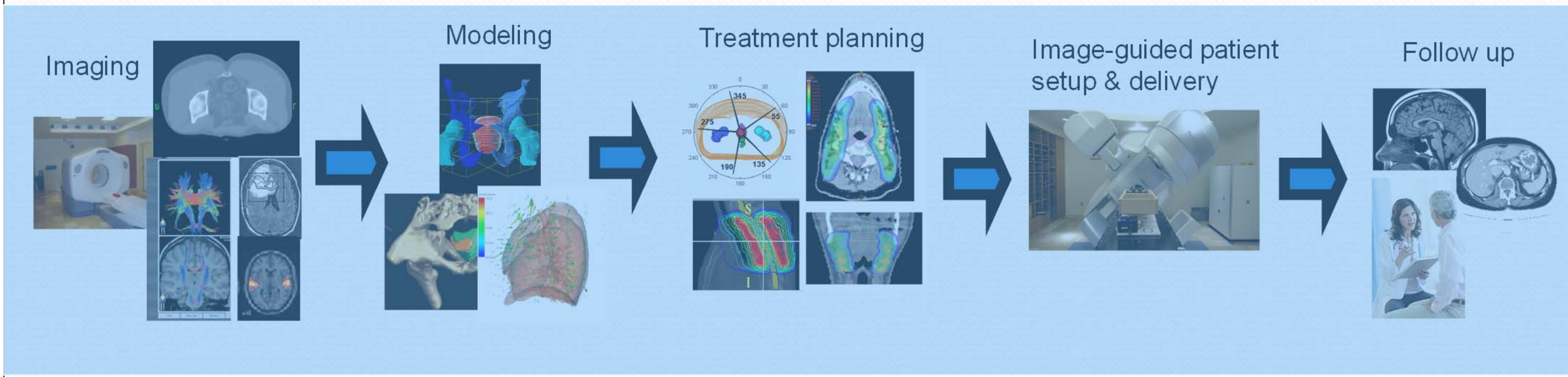

Image reconstruction	OAR segmentation	Supervised planning	Monoscopic imaging	Therapeutic response
High dimensional imaging	Tumor detection & segmentation	Unsupervised	Stereoscopic imaging	Survival
Sparsification compression	Image registration	Reimforcement learning	Cone beam CT	Toxity

ML for Medical Image Analysis

- Images reconstruction – low dose CT, fast MRI
- Imaging is one of the first choices for clinical diagnosis
- 70% clinical decisions depend on medical images

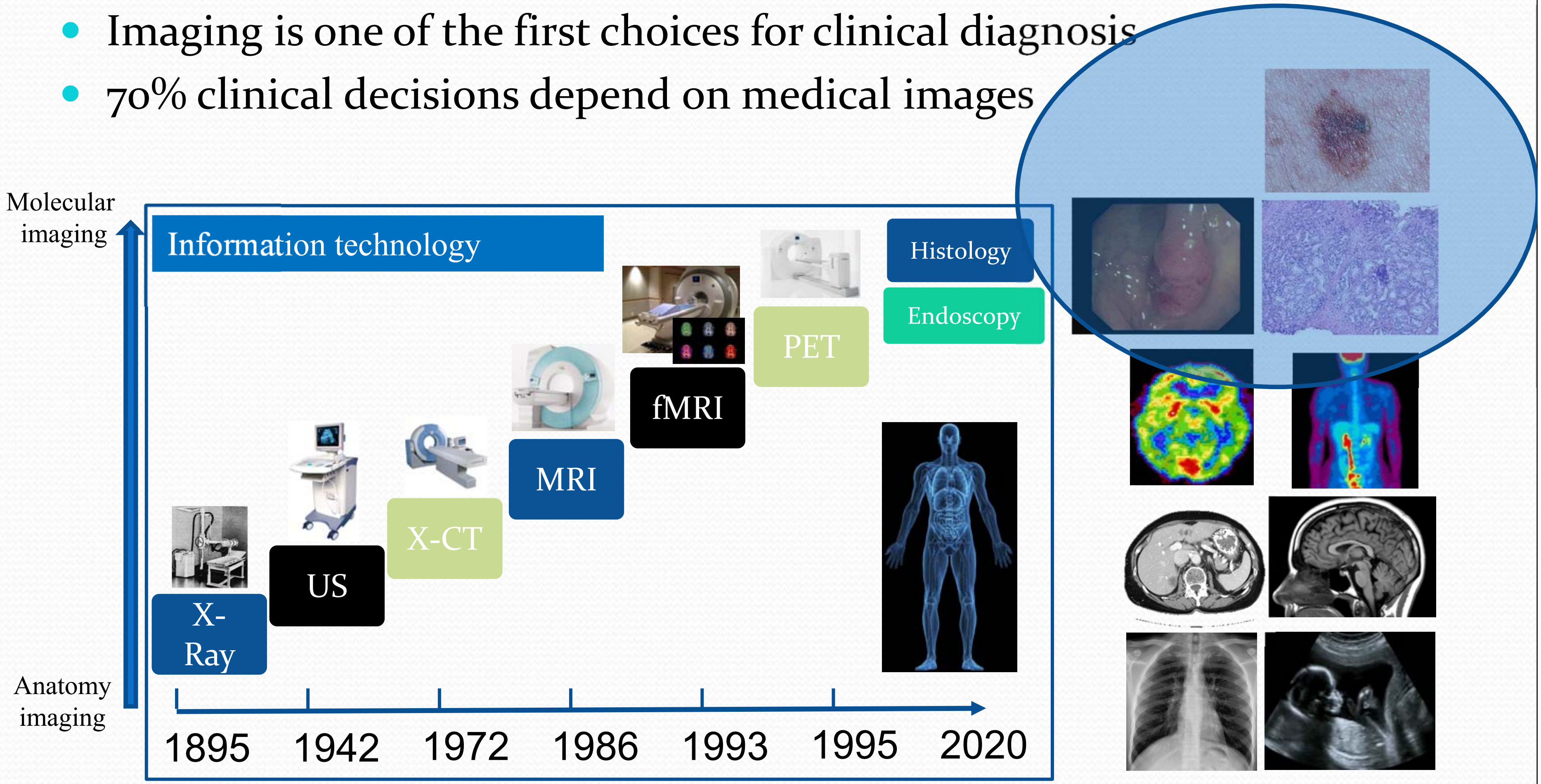

F |vwrvfrs|#Ip djbj#Dwhqwlrq Pds

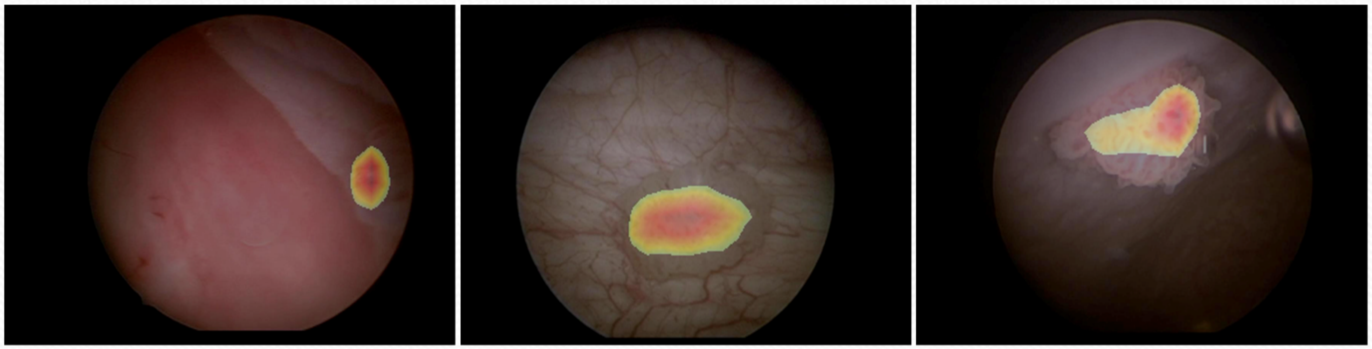

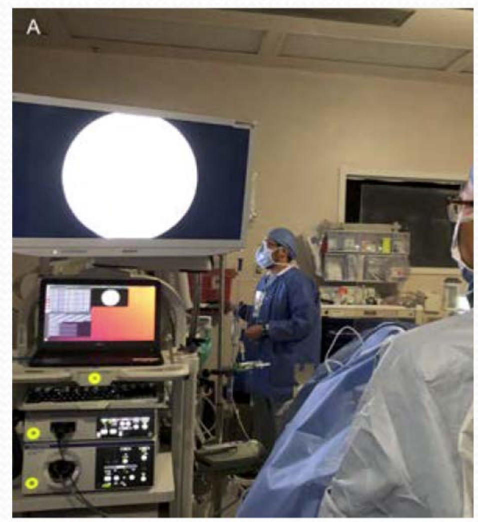

- We can directly visualize the network's attention when processing an input video.
- The discriminative regions of tumor are highlighted, suggesting the model works as expected and is able to identify tumors from artifacts and background.

E. Shkolyar, X. Jia, T.C. Chang, D. Trivedi, K. E. Mach, M. Meng, L. Xing, J. Liao, European Urology 76, 714-718, 2019

Image-based prostate cancer classification & virtual biopsy

- Importance
  - Different cancer levels (Gleason score) lead to different therapy
  - Reduce the core needle biopsy

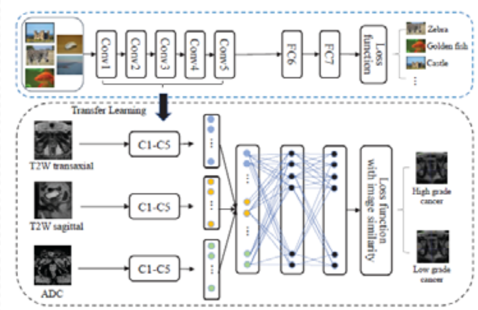

- Modality for diagnosis
  - Magnetic Resonance Imaging (MRI)

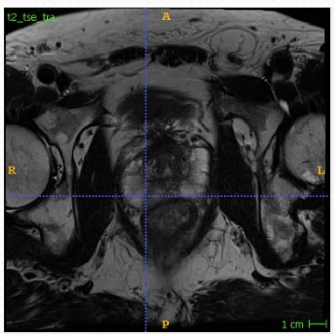

T2-weighted images (transaxial)

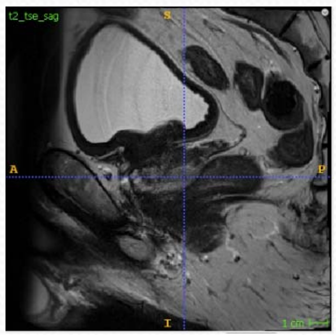

T2-weighted images (sagittal)

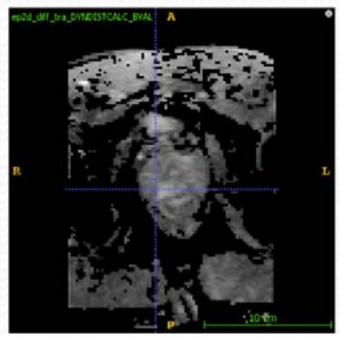

Apparent **D**iffusion **C**oefficient images

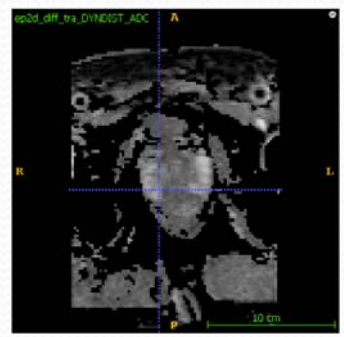

T1-weighted Contrast images

Y. Yuan, W. Qin, B. Han, et al, Medical Physics, 2019

CT/CBCT artifacts removal

Projection-domain scatter correction for cone beam computed tomography using a residual convolutional neural network

Yusuke Nomura[a)]
Department of Radiation Oncology, Faculty of Medicine and Graduate Sch
060-8638, Japan

Qiong Xu*
Global Station for Quantum Medical Science and Engineering, Global Insti
(GI-CoRE), Hokkaido University, Sapporo 060-8648, Japan

Hiroki Shirato
Global Station for Quantum Medical Science and Engineering, Global Insti
(GI-CoRE), Hokkaido University, Sapporo 060-8648, Japan
Department of Radiation Medicine, Faculty of Medicine and Graduate Scho
060-8638, Japan

Shinichi Shimizu
Global Station for Quantum Medical Science and Engineering, Global Insti
(GI-CoRE), Hokkaido University, Sapporo 060-8648, Japan
Department of Radiation Medical Science and Engineering, Faculty of Med
University, Sapporo 060-8638, Japan

Lei Xing[a)]
Global Station for Quantum Medical Science and Engineering, Global Insti
(GI-CoRE), Hokkaido University, Sapporo 060-8648, Japan
Department of Radiation Oncology, Stanford University, Stanford, CA, USA

(Received 12 December 2018; revised 8 April 2019; accepted for pul
published xx xxxx xxxx)

Purpose: Scatter is a major factor degrading the image quality of c
(CBCT). Conventional scatter correction strategies require handcr
hoc assumptions, which often leads to less accurate scatter remova
effective scatter correction method using a residual convolutional ne

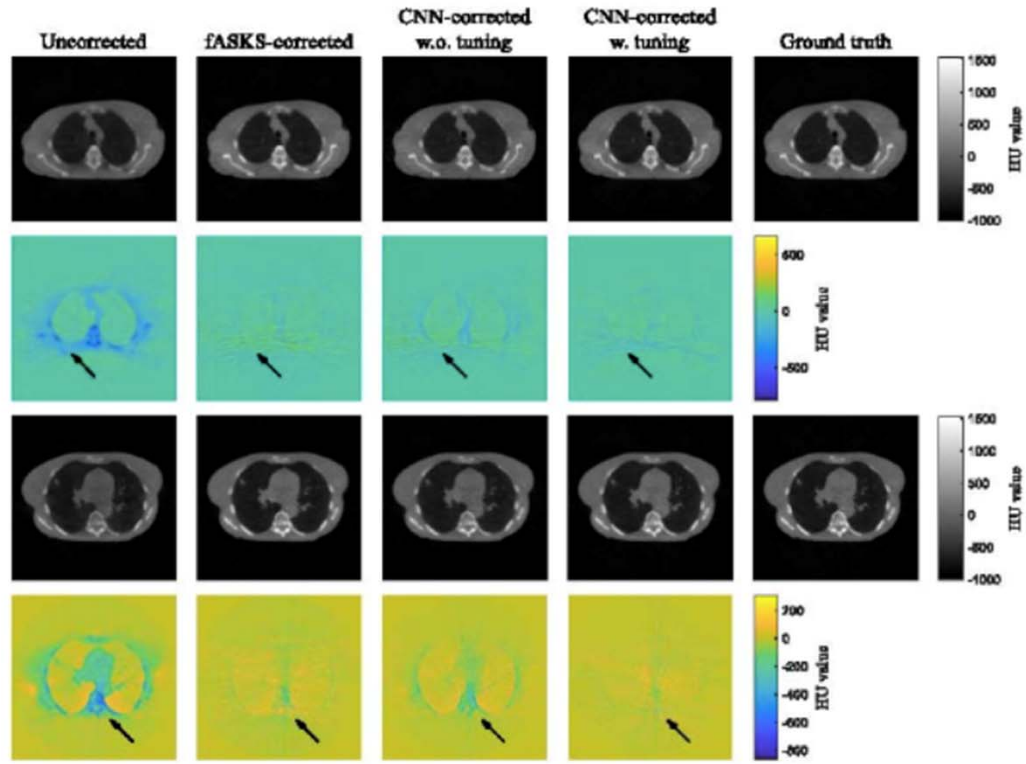

Dual-energy CT imaging using deep learning (Full 3D Meeting, 2019)

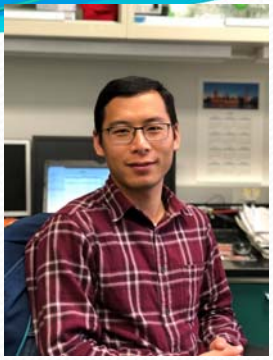

The HU difference between the predicted and original high-energy CT images are 3.47 HU, 2.95 HU, 2.38 HU and 2.40 HU for ROIs on spine, aorta, liver and stomach, respectively.

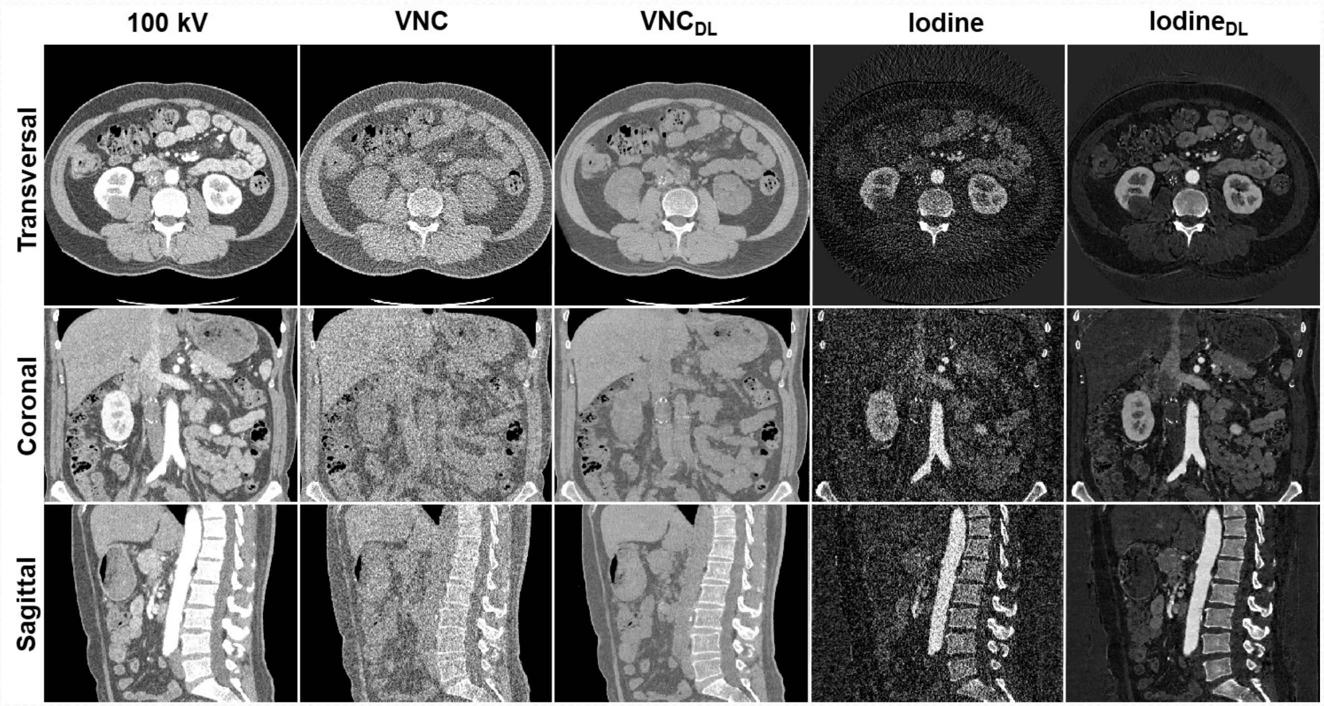

From super-resolution imaging to super resolution dose calculation

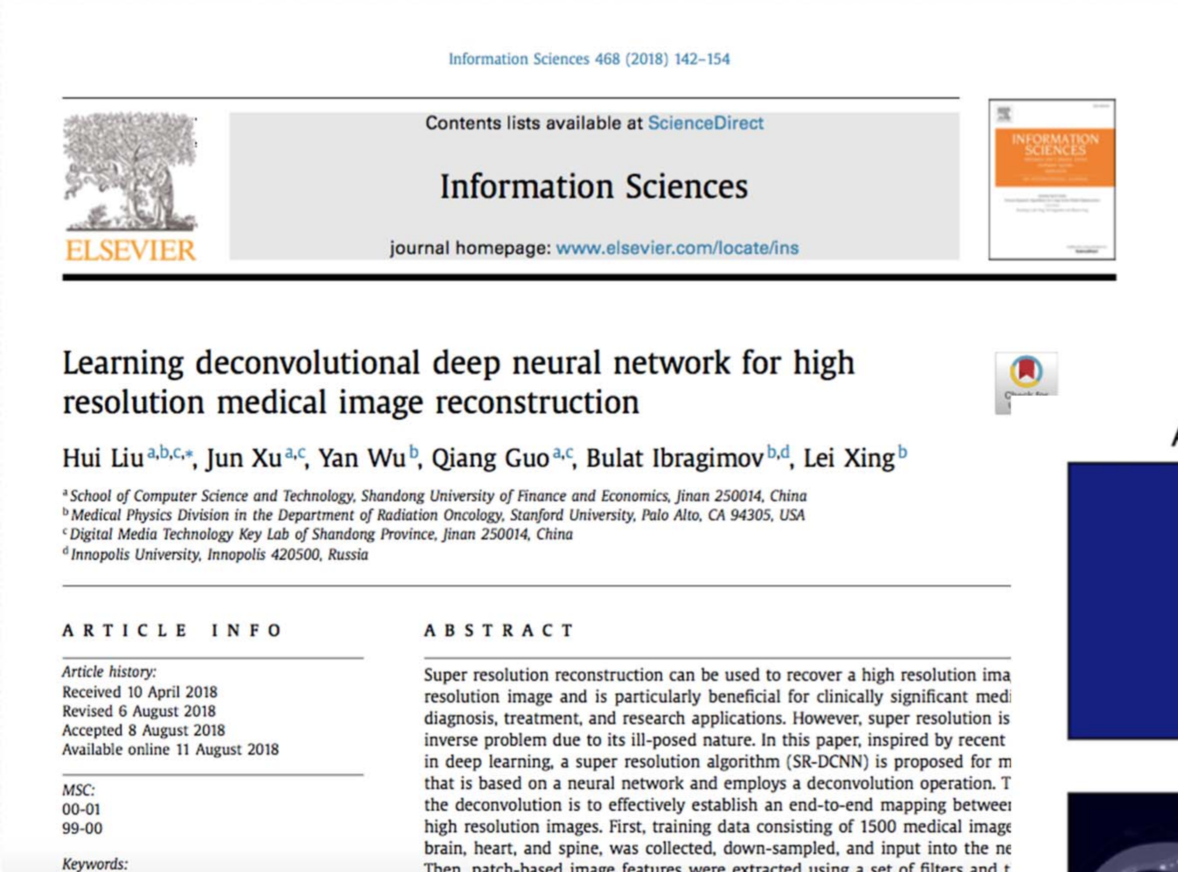
Information Sciences 468 (2018) 142–154

Contents lists available at ScienceDirect

Information Sciences

journal homepage: www.elsevier.com/locate/ins

ELSEVIER

Learning deconvolutional deep neural network for high resolution medical image reconstruction

Hui Liu[a,b,c,*], Jun Xu[a,c], Yan Wu[b], Qiang Guo[a,c], Bulat Ibragimov[b,d], Lei Xing[b]

[a] School of Computer Science and Technology, Shandong University of Finance and Economics, Jinan 250014, China
[b] Medical Physics Division in the Department of Radiation Oncology, Stanford University, Palo Alto, CA 94305, USA
[c] Digital Media Technology Key Lab of Shandong Province, Jinan 250014, China
[d] Innopolis University, Innopolis 420500, Russia

A R T I C L E I N F O

Article history:
Received 10 April 2018
Revised 6 August 2018
Accepted 8 August 2018
Available online 11 August 2018

MSC:
00-01
99-00

Keywords:

A B S T R A C T

Super resolution reconstruction can be used to recover a high resolution ima
resolution image and is particularly beneficial for clinically significant medi
diagnosis, treatment, and research applications. However, super resolution is
inverse problem due to its ill-posed nature. In this paper, inspired by recent
in deep learning, a super resolution algorithm (SR-DCNN) is proposed for m
that is based on a neural network and employs a deconvolution operation. T
the deconvolution is to effectively establish an end-to-end mapping betwee
high resolution images. First, training data consisting of 1500 medical image
brain, heart, and spine, was collected, down-sampled, and input into the ne
Then, patch-based image features were extracted using a set of filters and t

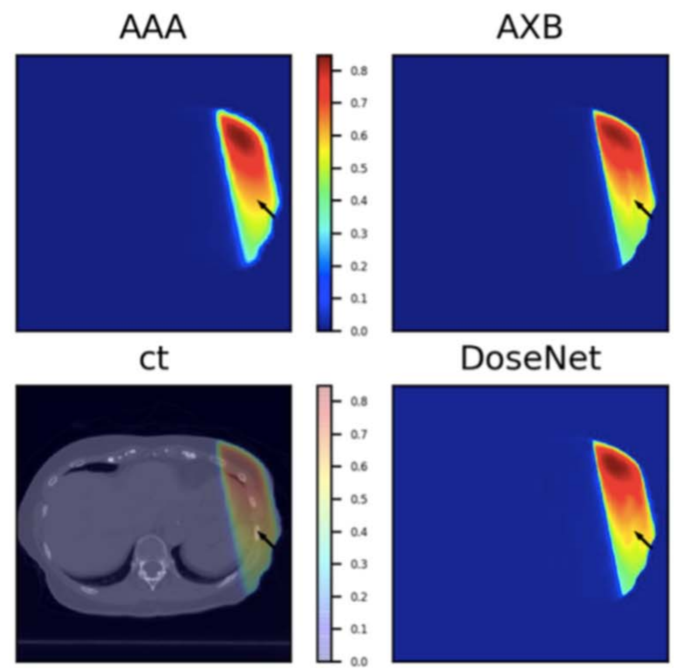

Super-resolution dose transformation and machine learning-based dose calculation

low resolution dose → DL model → high resolution dose

low cost algorithm & low resolution → DL model → high resolution dose, highly accurate algorithm

ultra-low cost algorithm & low resolution → DL model → high resolution dose, highly accurate algorithm

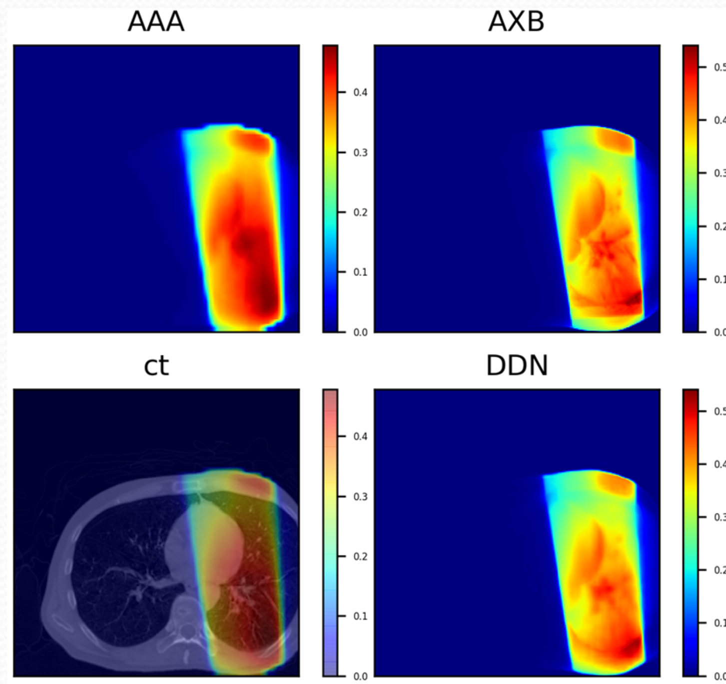

P. Dong & L. Xing, Deep DoseNet: a deep neural network for accurate dosimetric transformation between different spatial resolutions and/or different dose calculation algorithms for precision radiation therapy, Phys. Med. Biol., 2019

1. Nomura Y, Wang J, Shirato H, Shimizu S, Xing L, Fast spot-scanning proton dose calculation method with uncertainty quantification using a three-dimensional convolutional neural network, PMB Jun. 2020

Machine learning provides a new way for small field dosimetry and plan QA

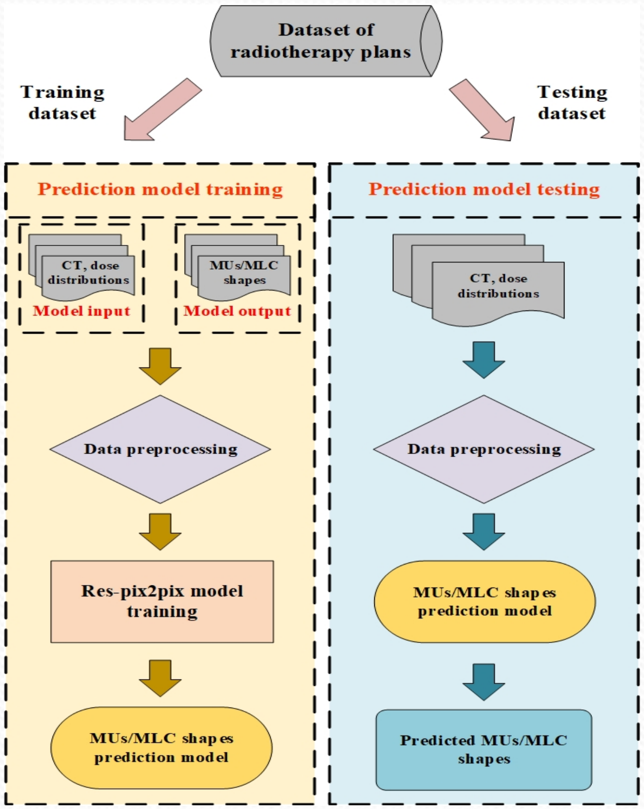

J. Fan, L. Xing, Y. Yang, under review

Output factor prediction

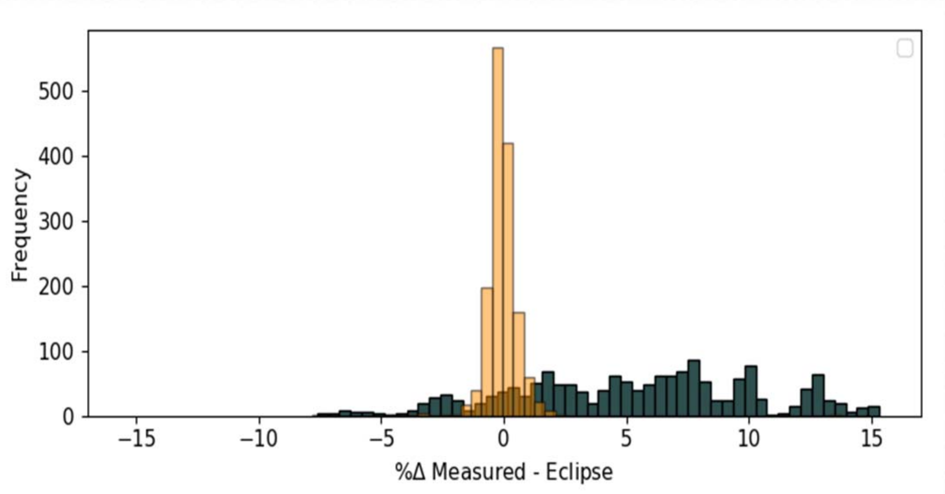

E. Schueler, W. Zhao, et al, in preparation

CT Imaging

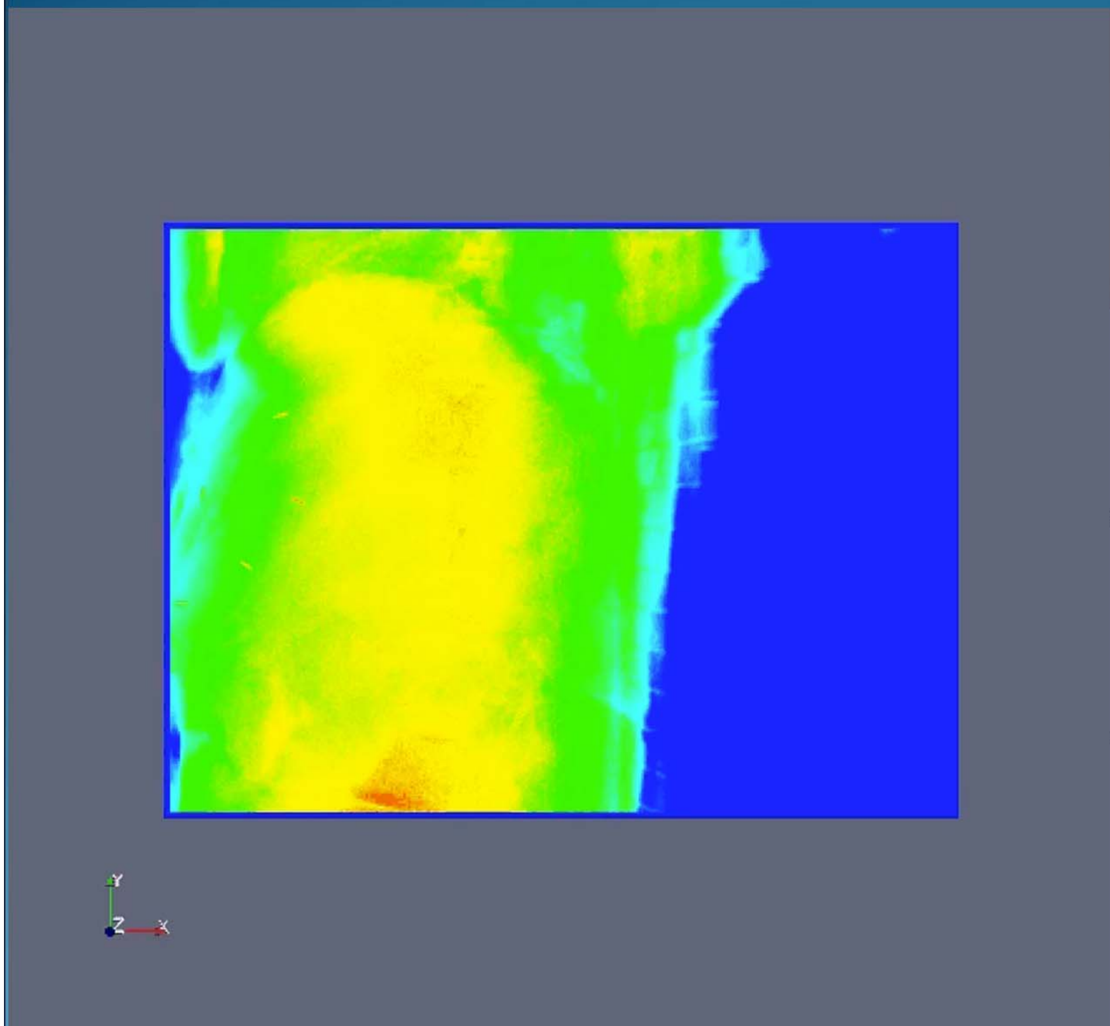

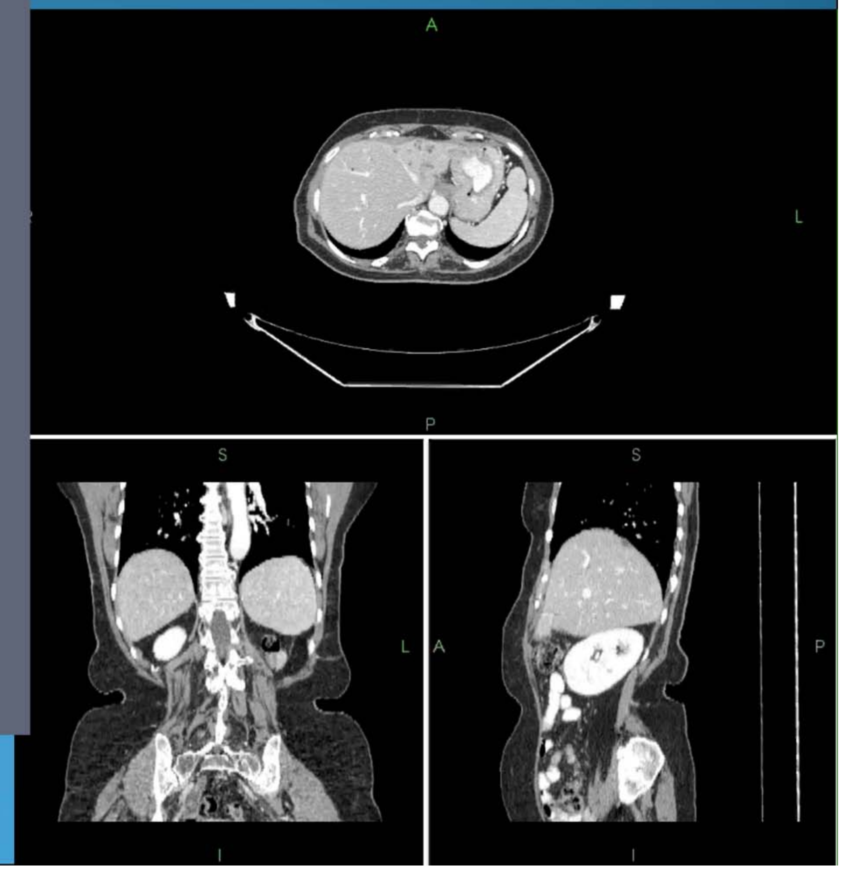

Pushing the sparsity to the limit -

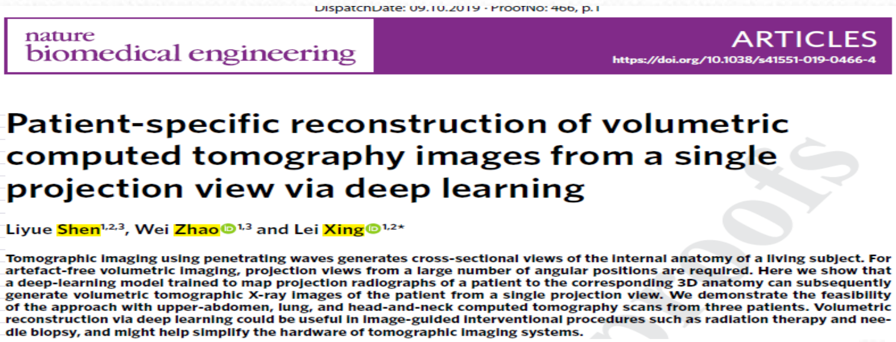
DispatchDate: 09.10.2019 · ProofNo: 466, p.1

nature biomedical engineering

ARTICLES

https://doi.org/10.1038/s41551-019-0466-4

Patient-specific reconstruction of volumetric computed tomography images from a single projection view via deep learning

Liyue Shen[1,2,3], Wei Zhao[1,3] and Lei Xing[1,2*]

Tomographic imaging using penetrating waves generates cross-sectional views of the internal anatomy of a living subject. For artefact-free volumetric imaging, projection views from a large number of angular positions are required. Here we show that a deep-learning model trained to map projection radiographs of a patient to the corresponding 3D anatomy can subsequently generate volumetric tomographic X-ray images of the patient from a single projection view. We demonstrate the feasibility of the approach with upper-abdomen, lung, and head-and-neck computed tomography scans from three patients. Volumetric reconstruction via deep learning could be useful in image-guided interventional procedures such as radiation therapy and needle biopsy, and might help simplify the hardware of tomographic imaging systems.

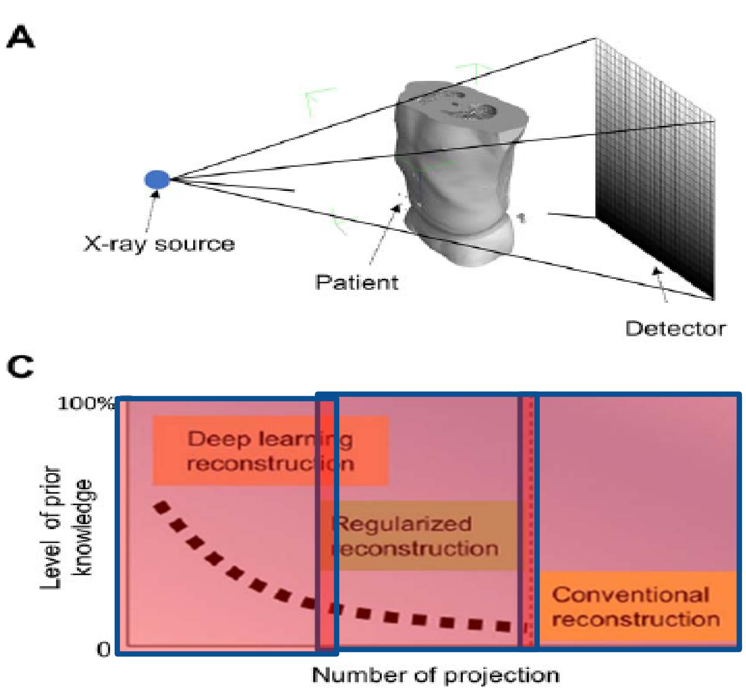

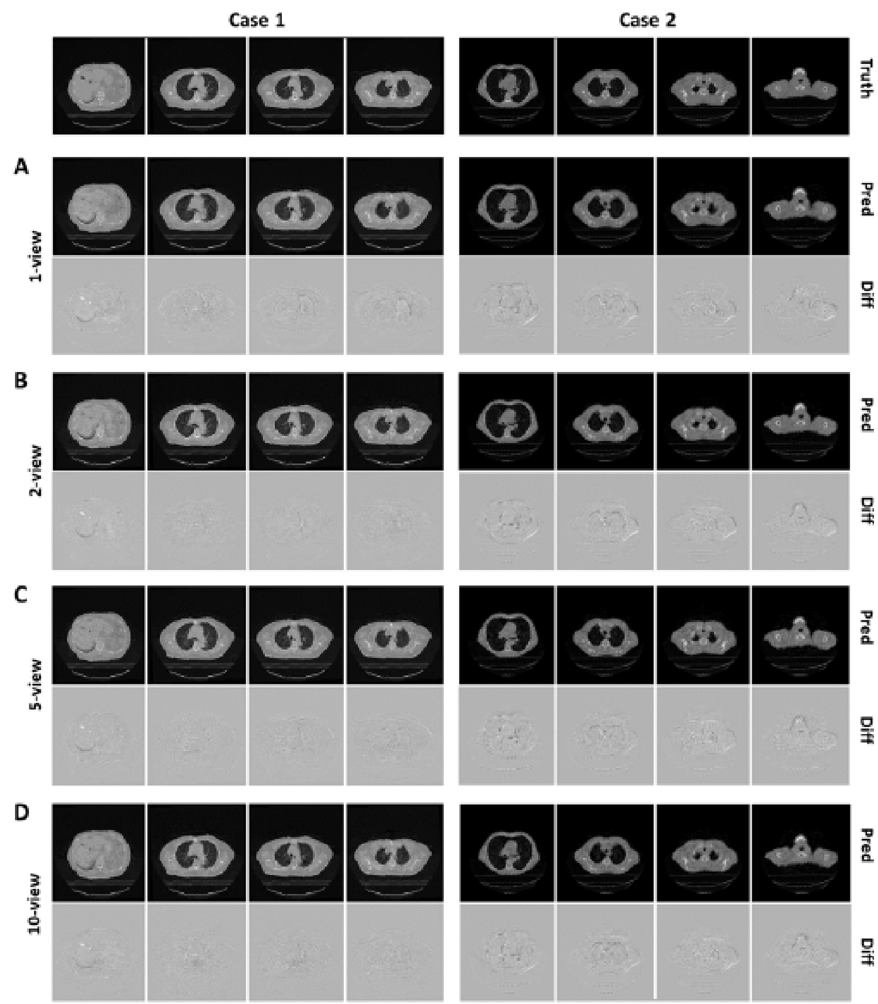

Shen L, Zhao W, Xing L, Nature Biomedical Engineering 3, 880-808, 2019

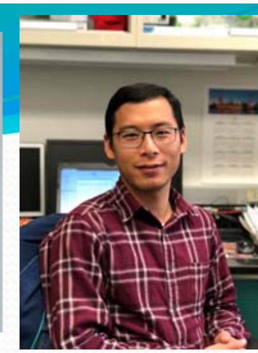

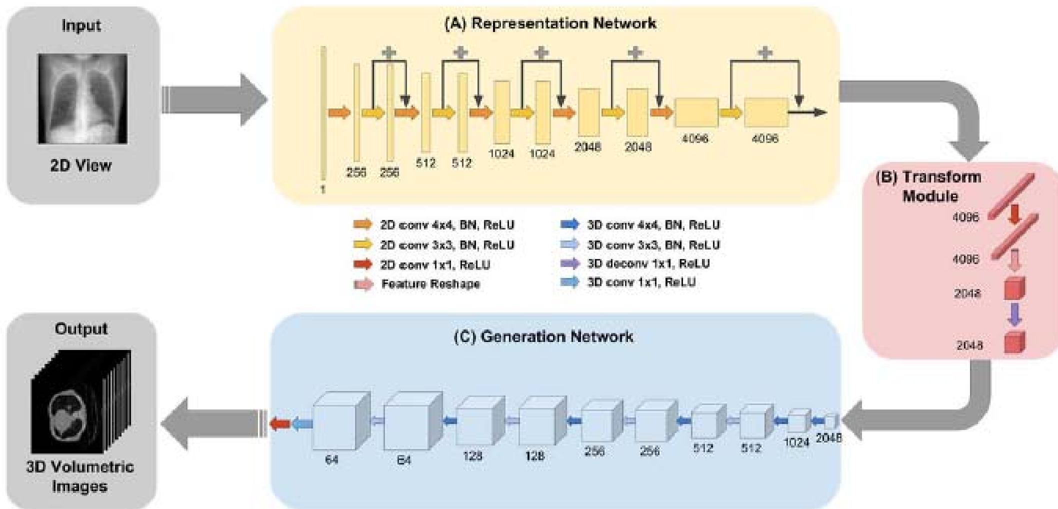

Fig. 2. Architecture of the proposed deep learning network. The input of the model is a single or multiple 2D projection(s). The representation network learns feature representation of physical structure from the input. The extracted 2D feature vector is reshaped and transferred by the transform module to 3D representation cube for subsequent reconstruction. The generation network utilizes representative features extracted in the former stages to generate the corresponding 3D volumetric images.

Shen L, Zhao W, Xing L, Nature Biomedical Engineering 3, 880-808, 2019

Sparse Data MR Image Reconstruction

Data Sampling

Raw data are sampled point by point in Fourier domain (k-space)

Image Reconstruction

Inverse Fourier transform is applied on the raw data to generate output in the image domain

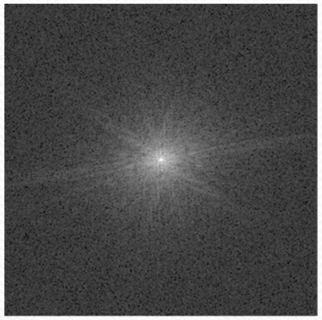

Inverse Fourier Transform

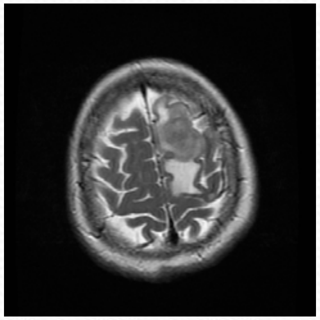

M. Mardani,…, L Xing, J Pauly, TMI, 2019
Y. Wu, et al, Mag. Res. Imag., 2019

Integrated MRI-Radiotherapy Systems:
MRI Guided Localization & Delivery

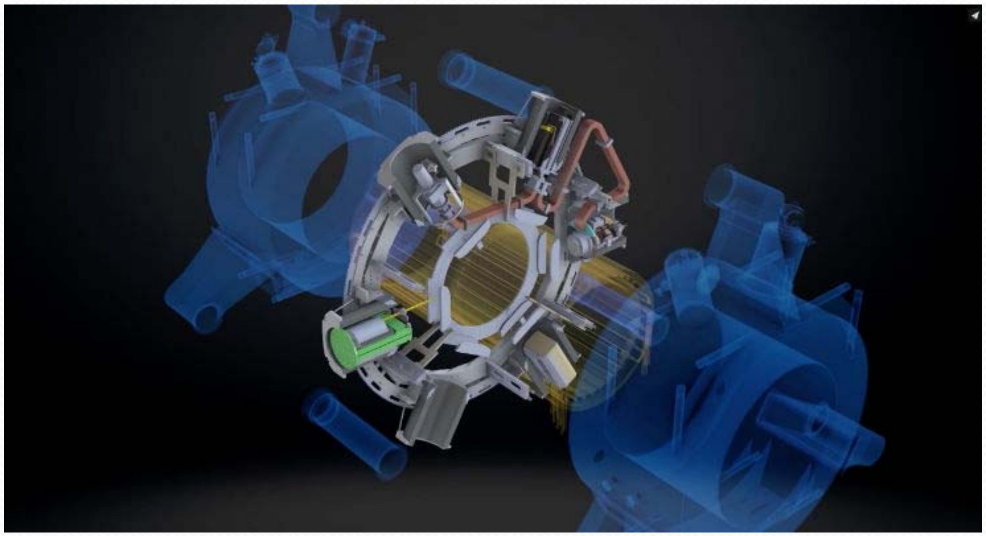

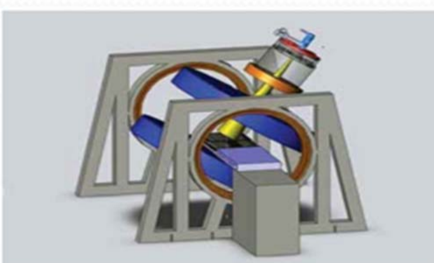

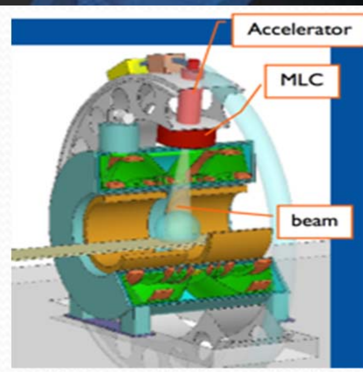

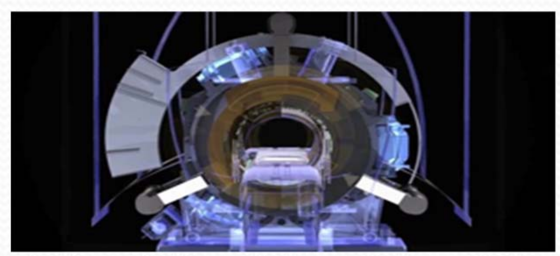

Segmentation of organs-at-risks in head and neck CT images using convolutional neural networks

Bulat Ibragimov[a)] and Lei Xing
Department of Radiation Oncology, Stanford University School of Medicine, Stanford, California 94305, USA

(Received 2 May 2016; revised 31 October 2016; accepted for publication 23 November 2016; published 13 February 2017)

Purpose: Accurate segmentation of organs-at-risks (OARs) is the key step for efficient planning of radiation therapy for head and neck (HaN) cancer treatment. In the work, we proposed the first deep learning-based algorithm, for segmentation of OARs in HaN CT images, and compared its performance against state-of-the-art automated segmentation algorithms, commercial software, and server variability.

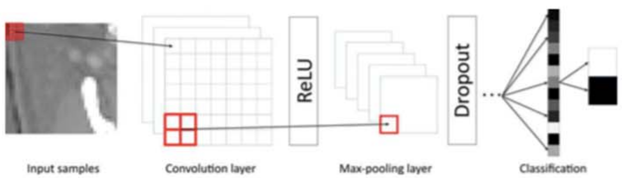

FIG. 1. A schematic illustration of the convolutional neural network architecture. Three orthogonal cross-sections around target voxel define the input of the network that consists of three stacks of convolution, ReLU, max-pooling layer, and dropout layers, fully connected and softmax layers. [Color figure can be viewed at wileyonlinelibrary.com]

Medical Physics, 44 (2), February 2017

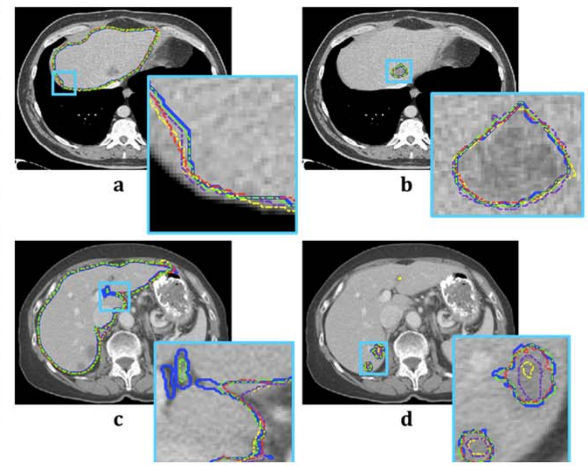

#1 in the Liver Tumor Segmentation Challenge (LiTS-ISBI2017)

- H. Seo, R. Xiao, L. Xing

Score	Liver			
	SBBS-CNN	Dual-frame U-Net	Atrous CNN /pyramid pooling	Proposed Network
DSC (%)	97.18 ± 1.22	97.46 ± 1.29	97.89 ± **1.01**	**98.77** ± 1.03
VOE (%)	5.81 ± 2.48	5.05 ± 2.29	3.71 ± 2.25	**3.10 ± 2.01**
RVD (%)	0.91 ± 0.19	0.77 ± 0.14	0.33 ± **0.10**	**0.27 ± 0.10**
ASSD (mm)	1.80 ± 0.55	1.81 ± 0.56	1.06 ± 0.40	**0.92 ± 0.37**
MSSD (mm)	12.48 ± 5.12	13.75 ± 5.38	9.37 ± 3.99	**8.53 ± 3.65**

Table 1. Quantitative scores of the liver-segmentation results. All metric is described in detail in (30).

Autonomous treatment planning for RT

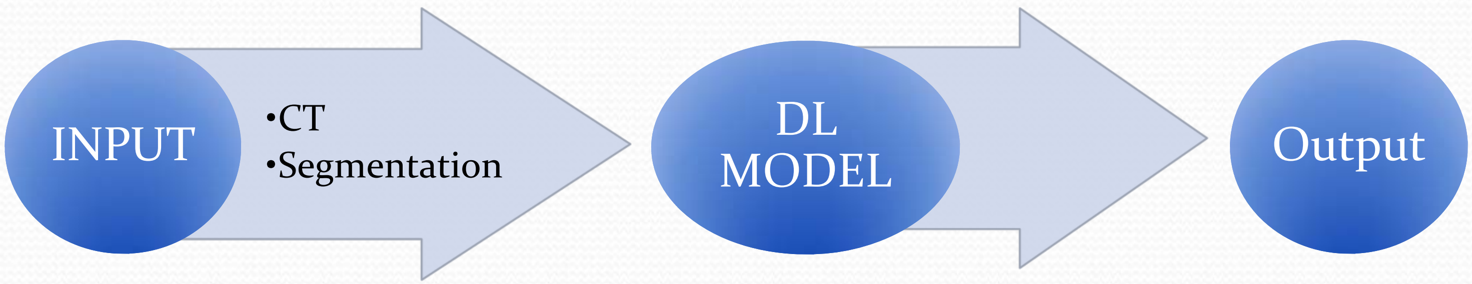

Clinical plan

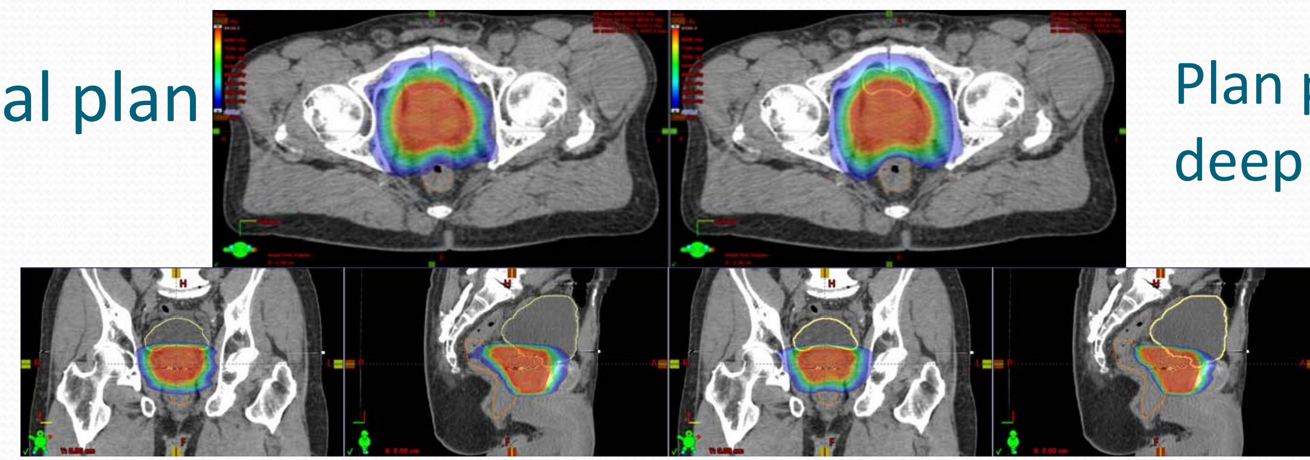

Plan predicted by deep learning

M. Ma, N. Kovalchuk, M. Buyyounouski, L. Xing, Y. Yang, Med Phys, 2019

Beam trajectory selection using reinforcement learning

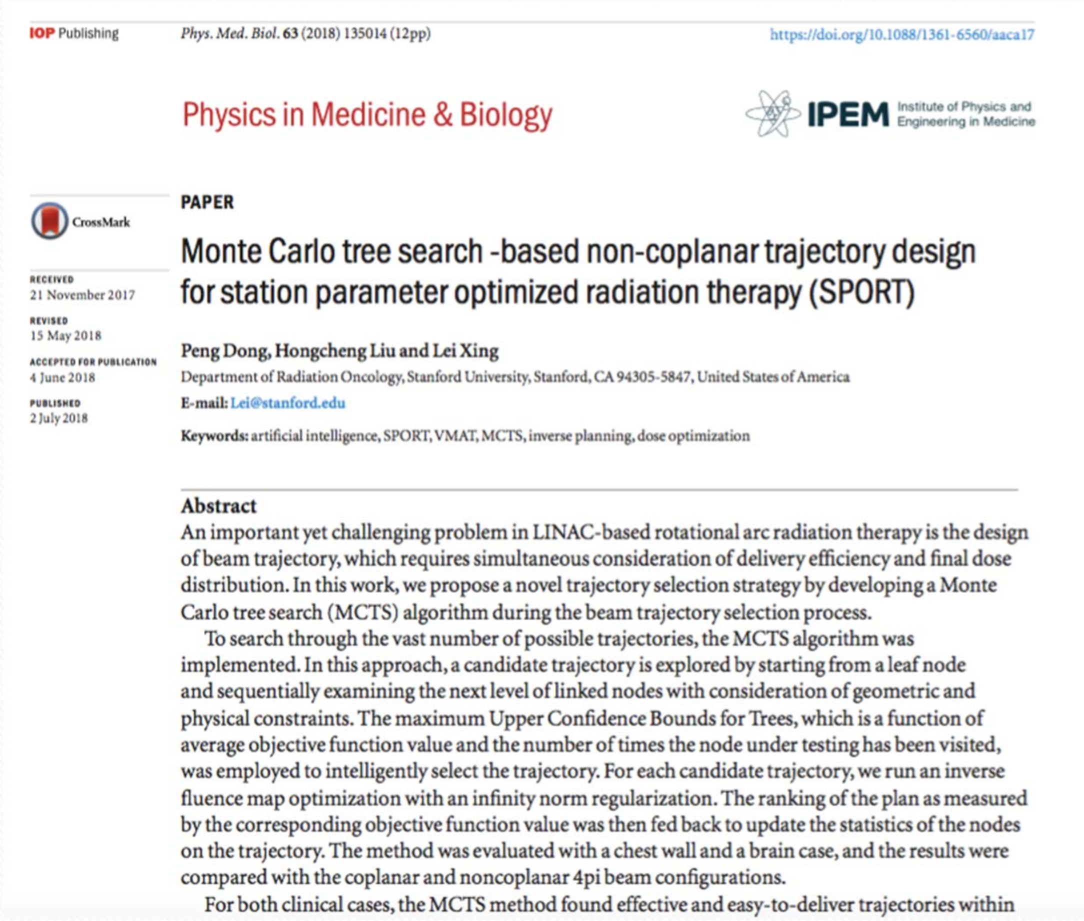

IOP Publishing | Phys. Med. Biol. 63 (2018) 135014 (12pp) | https://doi.org/10.1088/1361-6560/aaca17

Physics in Medicine & Biology | IPEM Institute of Physics and Engineering in Medicine

CrossMark

RECEIVED
21 November 2017

REVISED
15 May 2018

ACCEPTED FOR PUBLICATION
4 June 2018

PUBLISHED
2 July 2018

PAPER

Monte Carlo tree search -based non-coplanar trajectory design for station parameter optimized radiation therapy (SPORT)

Peng Dong, Hongcheng Liu and Lei Xing

Department of Radiation Oncology, Stanford University, Stanford, CA 94305-5847, United States of America

E-mail: Lei@stanford.edu

Keywords: artificial intelligence, SPORT, VMAT, MCTS, inverse planning, dose optimization

Abstract

An important yet challenging problem in LINAC-based rotational arc radiation therapy is the design of beam trajectory, which requires simultaneous consideration of delivery efficiency and final dose distribution. In this work, we propose a novel trajectory selection strategy by developing a Monte Carlo tree search (MCTS) algorithm during the beam trajectory selection process.

To search through the vast number of possible trajectories, the MCTS algorithm was implemented. In this approach, a candidate trajectory is explored by starting from a leaf node and sequentially examining the next level of linked nodes with consideration of geometric and physical constraints. The maximum Upper Confidence Bounds for Trees, which is a function of average objective function value and the number of times the node under testing has been visited, was employed to intelligently select the trajectory. For each candidate trajectory, we run an inverse fluence map optimization with an infinity norm regularization. The ranking of the plan as measured by the corresponding objective function value was then fed back to update the statistics of the nodes on the trajectory. The method was evaluated with a chest wall and a brain case, and the results were compared with the coplanar and noncoplanar 4pi beam configurations.

For both clinical cases, the MCTS method found effective and easy-to-deliver trajectories within

Kahn, Fahimian et al

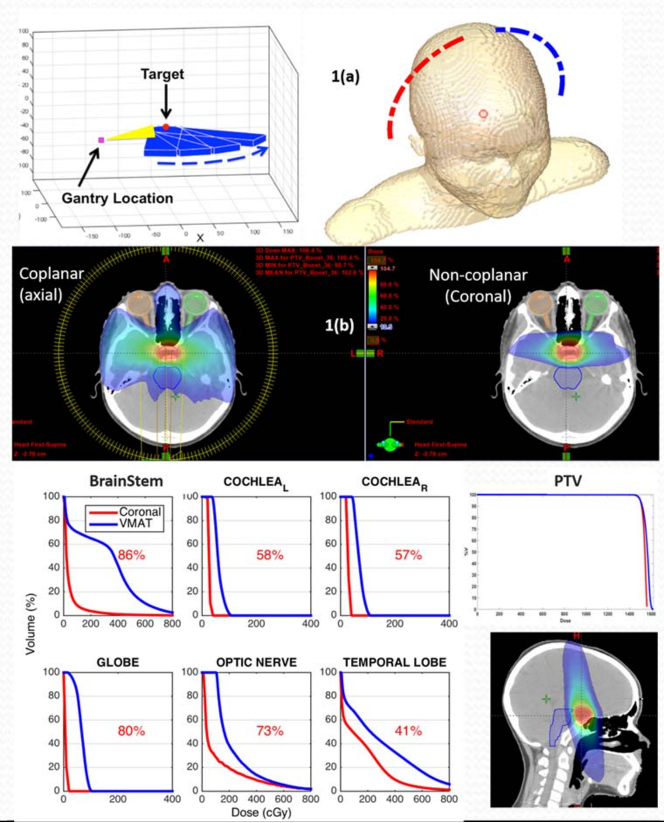

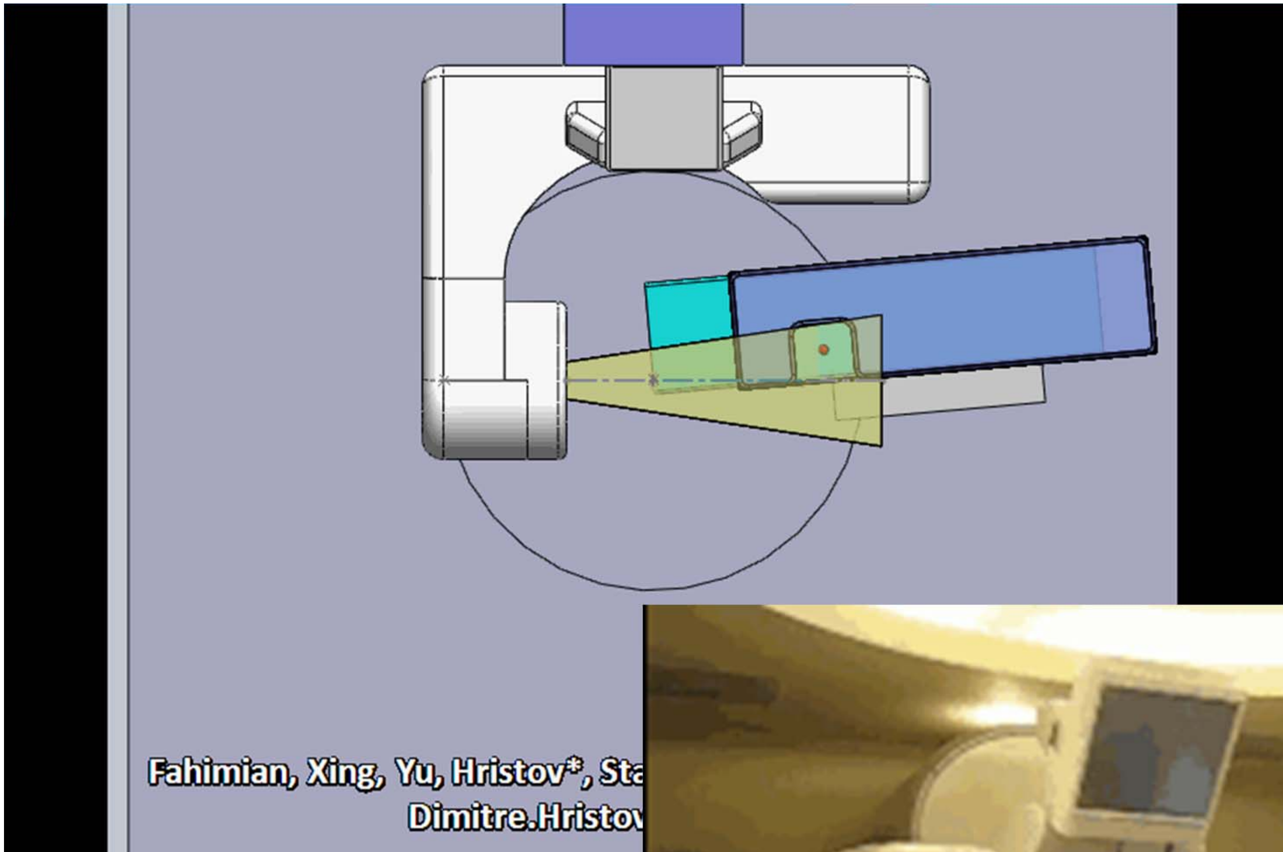
Fahimian, Xing, Yu, Hristov*,


Fahimian, Xing, Hristov*, Stanford University, US 61/493,977
Dimitre.Hristov@Stanford.edu

Beam level imaging

Stanford MEDICINE | Radiation Oncology Medical Physics

Landmark detection in cephalometric analysis

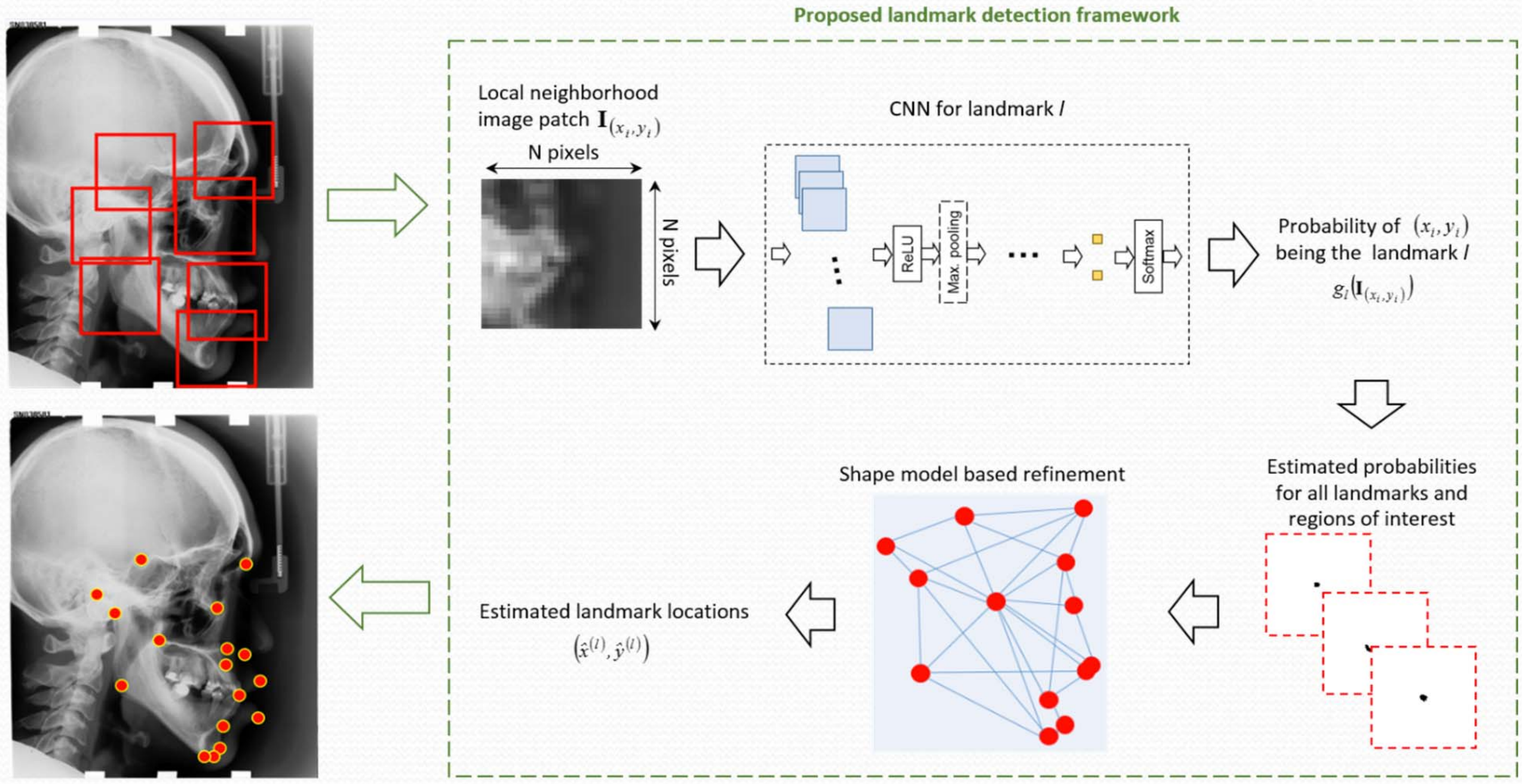

Stanford University
Department of Radiation Oncology
School of Medicine

Visualizing the invisible –

Deep learning-augmented IGRT

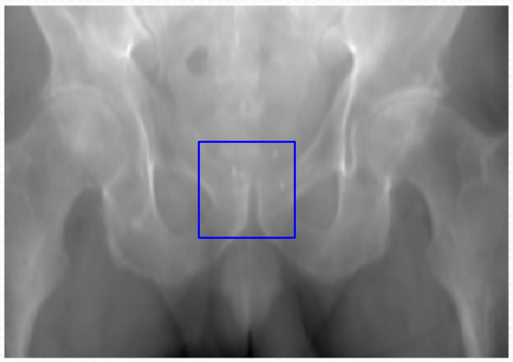

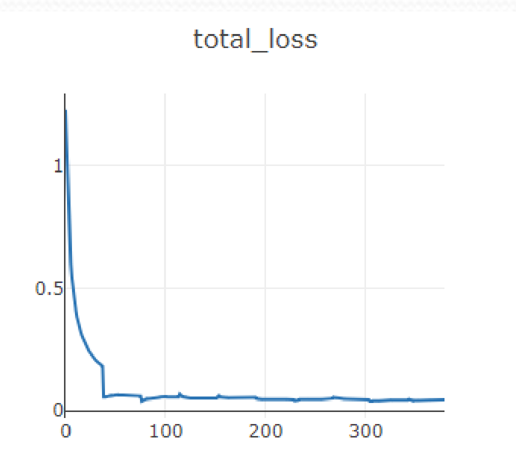

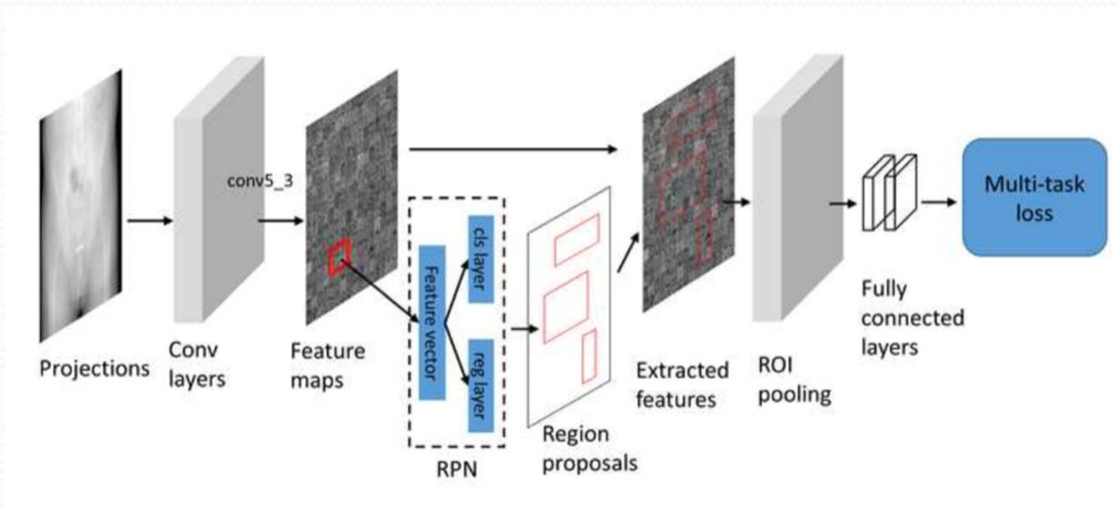

Zhao et al ,IJROBP, 2019

Target tracking

- Example of prostate motion tracking in AP direction
  - The predict prostate position match the ground truth quite well.

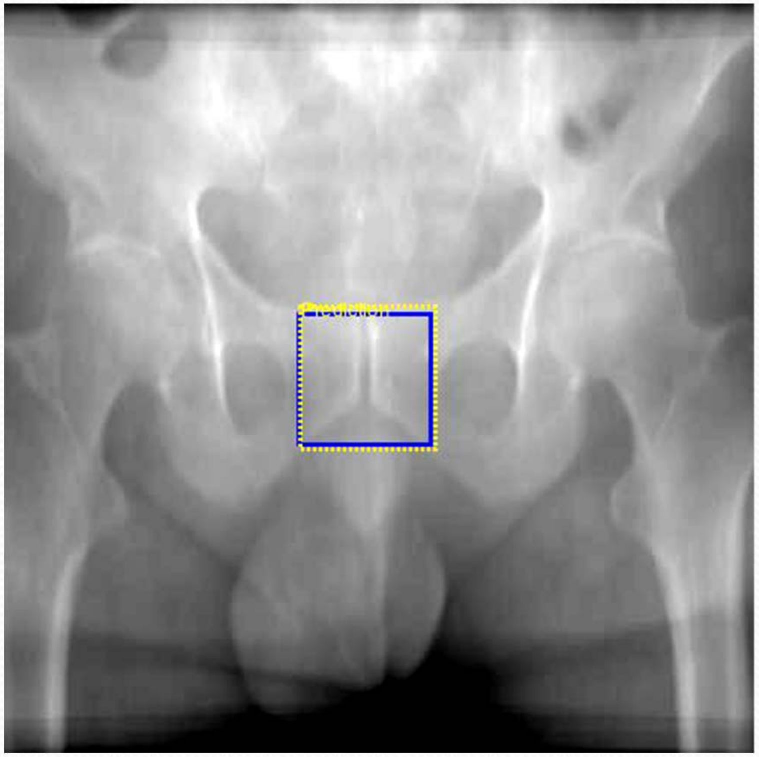

- Pancreas, lung, etc.

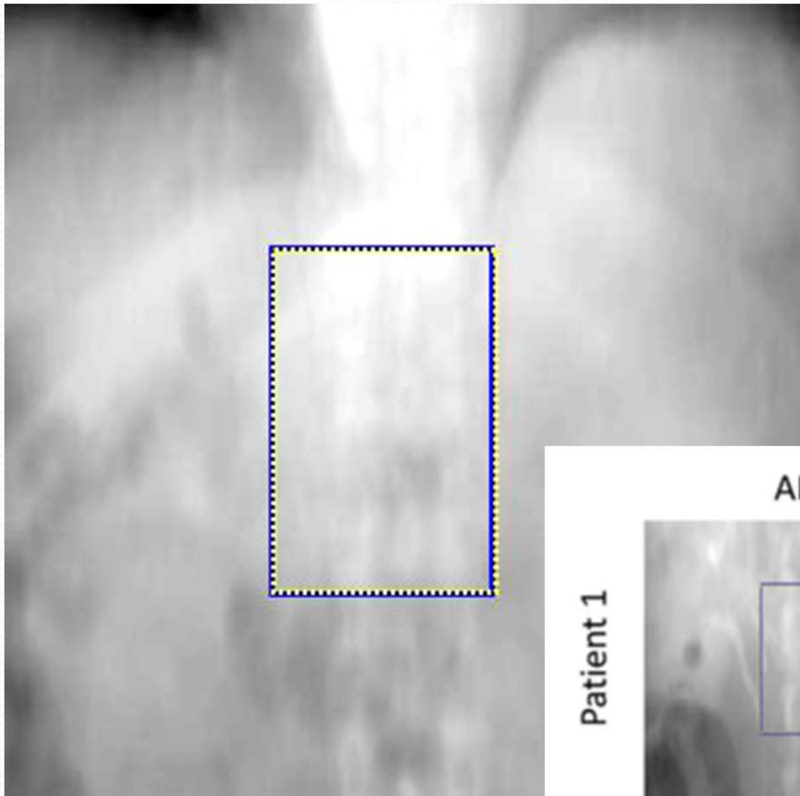

Ground truth

Predicted

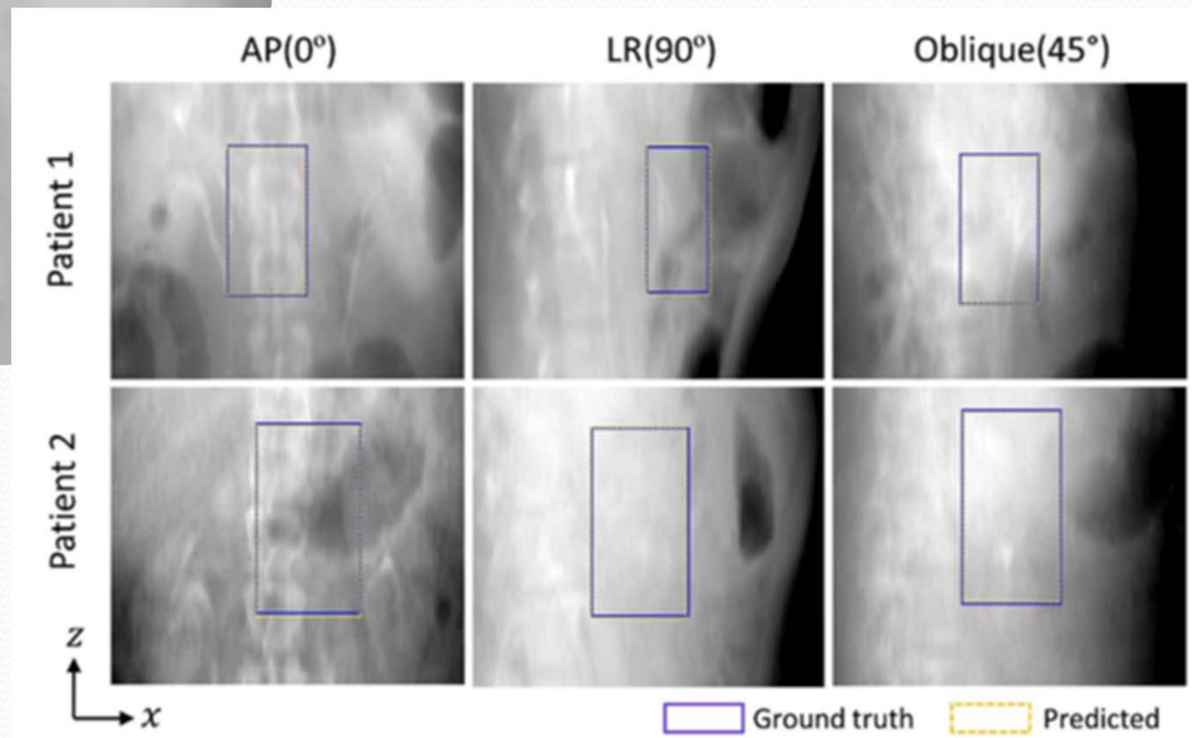

Tracking on PTV for pancreas radiotherapy

Zhao et al ,IJROBP, 2019

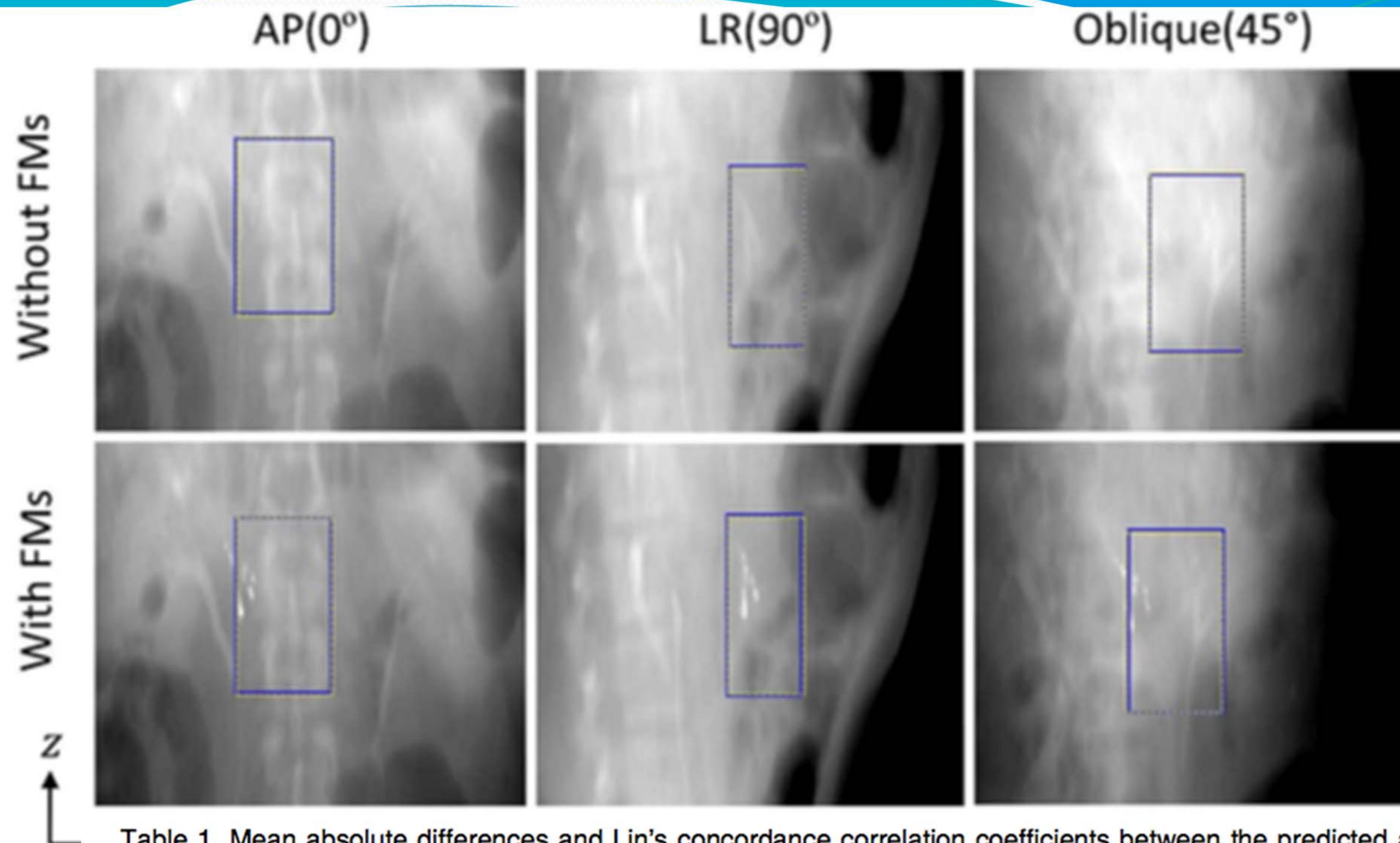

Table 1. Mean absolute differences and Lin's concordance correlation coefficients between the predicted and annotated PTV positions in anterior-posterior, left-right, and oblique directions. Data are shown as means±standard deviations.

Index	Anterior-posterior				Left-right				Oblique			
	MAD_x (mm)	ρ_c	MAD_z (mm)	ρ_c	MAD_x (mm)	ρ_c	MAD_z (mm)	ρ_c	MAD_x (mm)	ρ_c	MAD_z (mm)	ρ_c
1	1.95±0.75	0.94	2.55±1.28	0.95	0.46±0.48	0.99	0.97±0.64	0.98	0.74±0.64	0.98	1.49±1.14	0.97
2	1.49±1.53	0.95	2.41±1.86	0.94	0.60±2.21	0.94	0.38±1.31	0.95	1.02±0.72	0.98	2.25±1.44	0.95
wo/ FMs	1.36±0.65	0.97	1.41±1.48	0.97	0.34±0.41	0.99	1.32±0.92	0.98	0.68±0.68	0.98	1.31±0.89	0.98
w/ FMs	1.33±1.15	0.96	2.49±1.75	0.94	0.51±0.64	0.98	1.57±1.21	0.97	0.83±1.38	0.95	1.47±1.81	0.94

From population-average nomogram to deep learning-based toxicity prediction

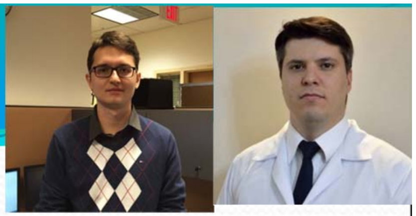

- B. Ibrambrov, D. Toesca, D. Chang, A Koong, L Xing

Current approach:

(i) NTCP/TCP types of modeling

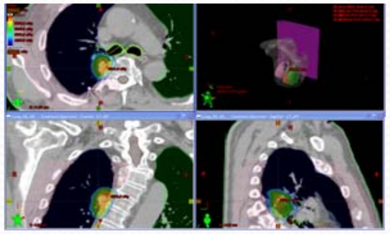

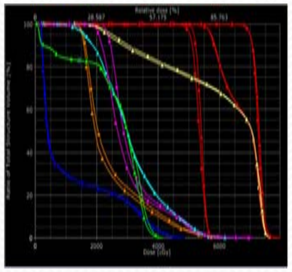

Predictive model

Problems: biological heterogeneity, spatial information

Deep dose-toxicity prediction

Multi-path network: 1) 3D CNN for dose plan; 2) fully-connected path for features

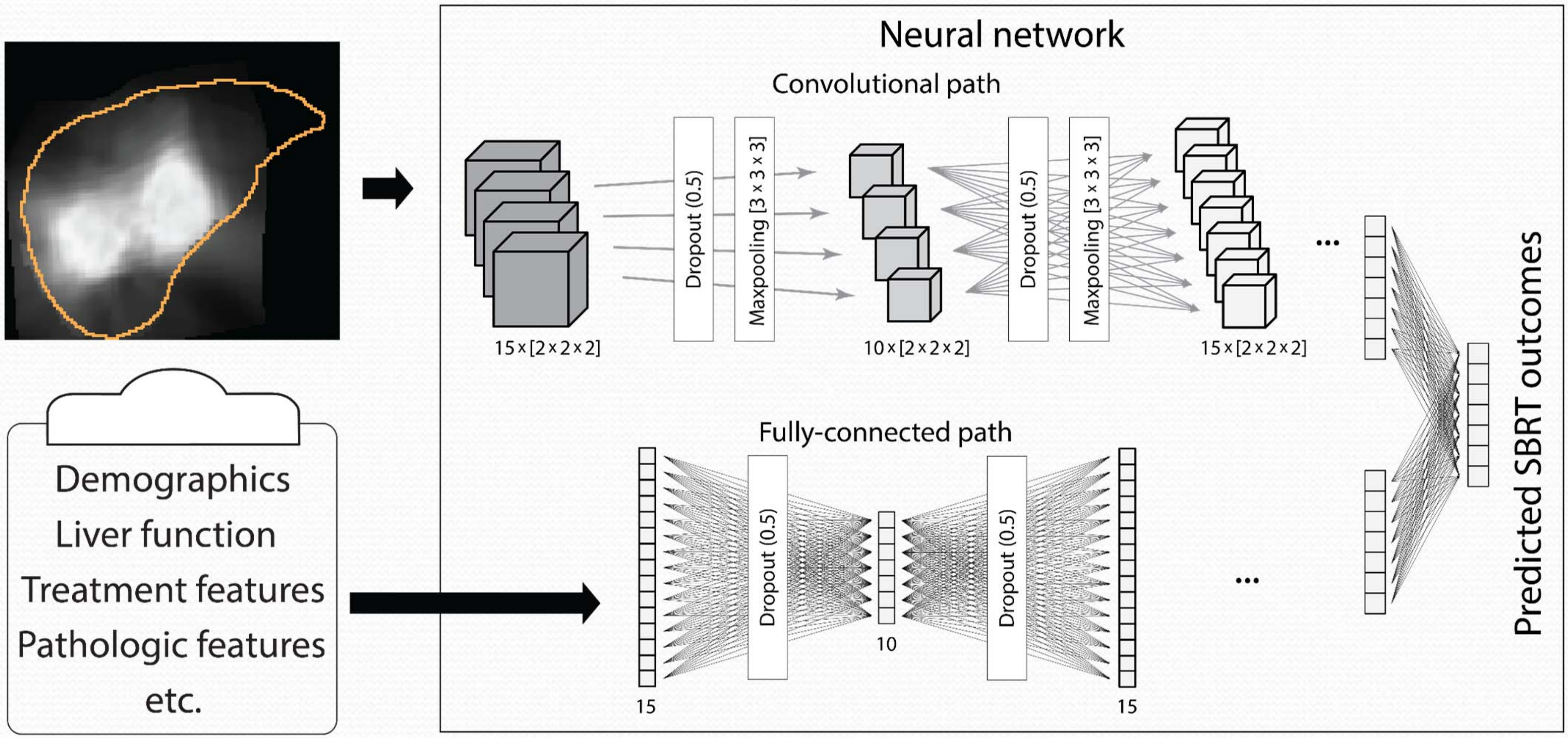

survival & toxicity results

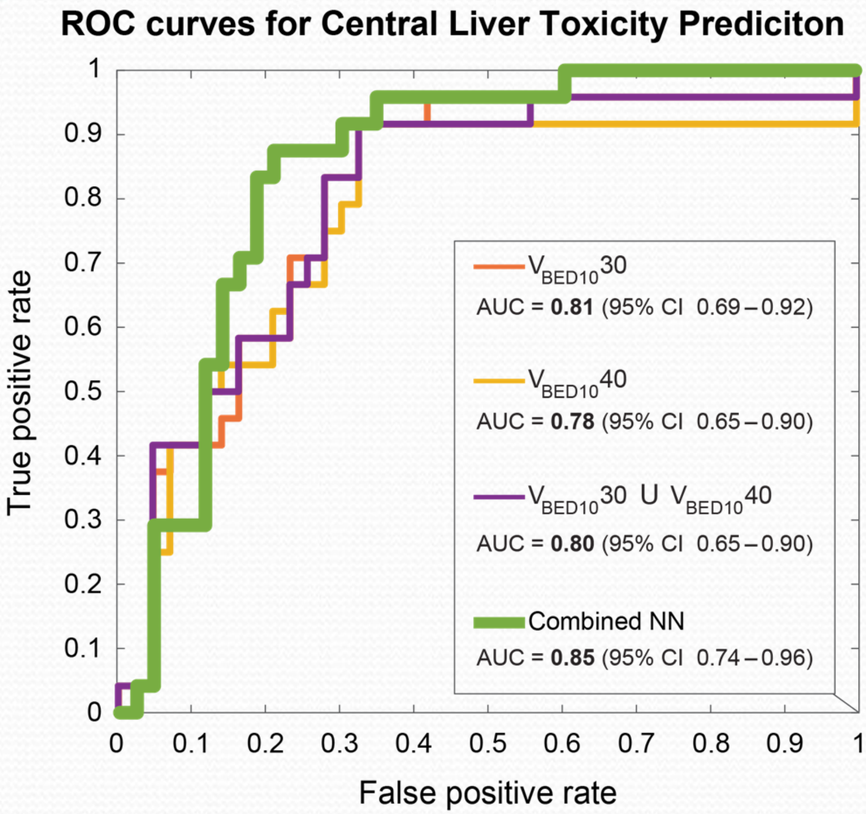

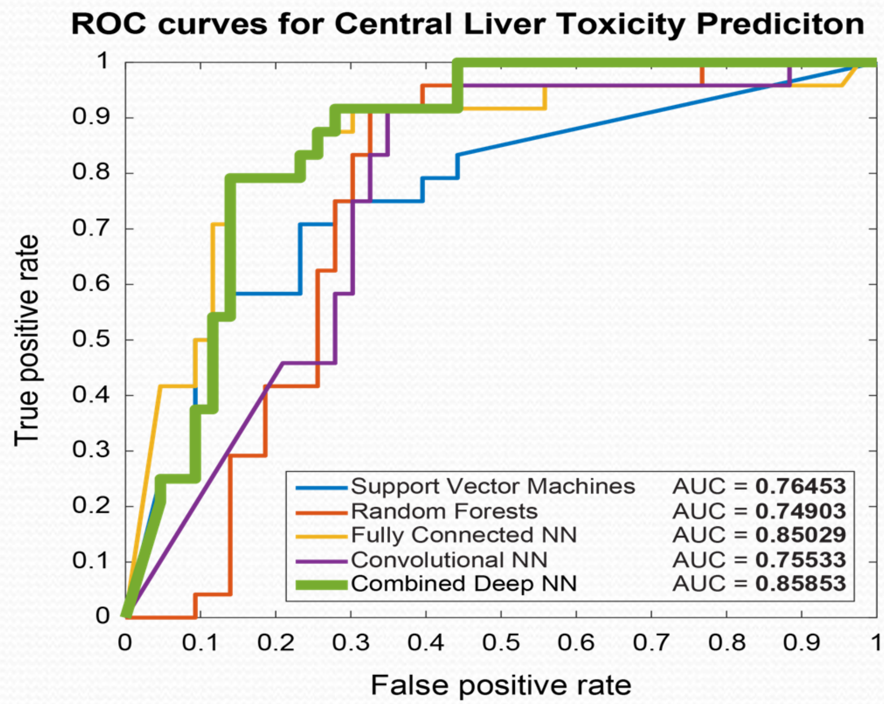

Magical deep learning box

Problem:

3D dose plan
+
Image analysis

Prediction

Data Dimension-Reduction

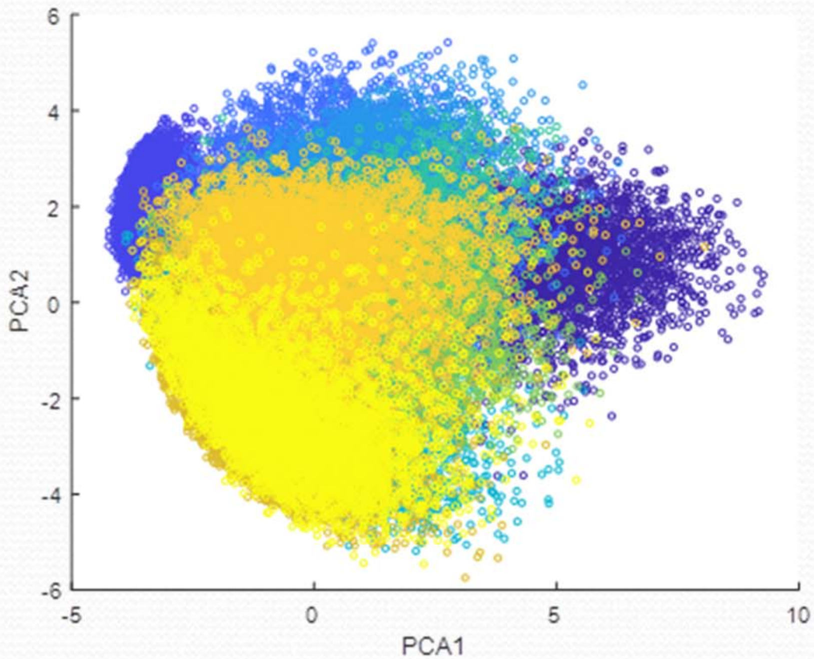

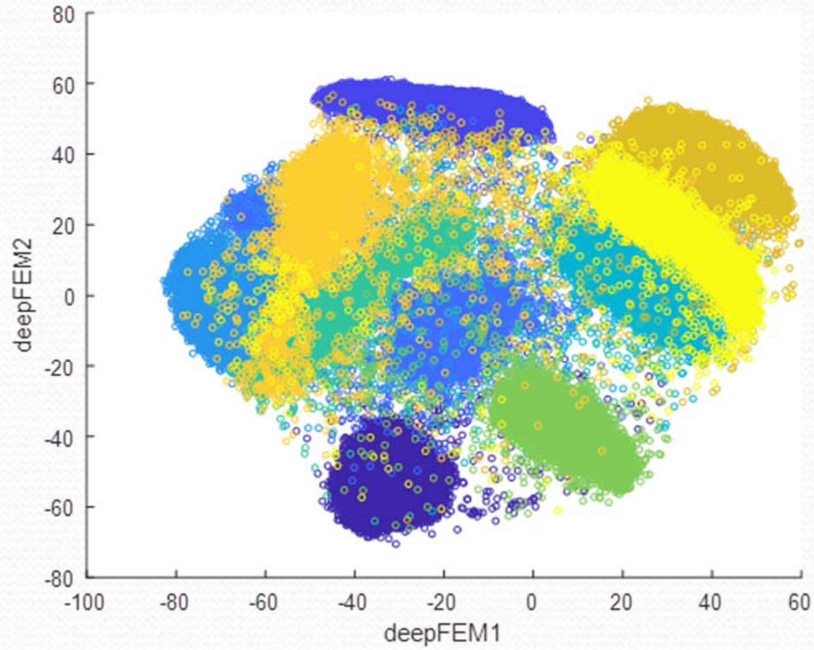

Islam T & Xing L, Nature Biomedical Engineering, under revision, 2020

On-going research

- Better AI models.
- Interpretable and trustworthy AI.
- General instead of task-specific AI.
- Data & annotation.
- Clinical implementation and workflow related issues.

Summary

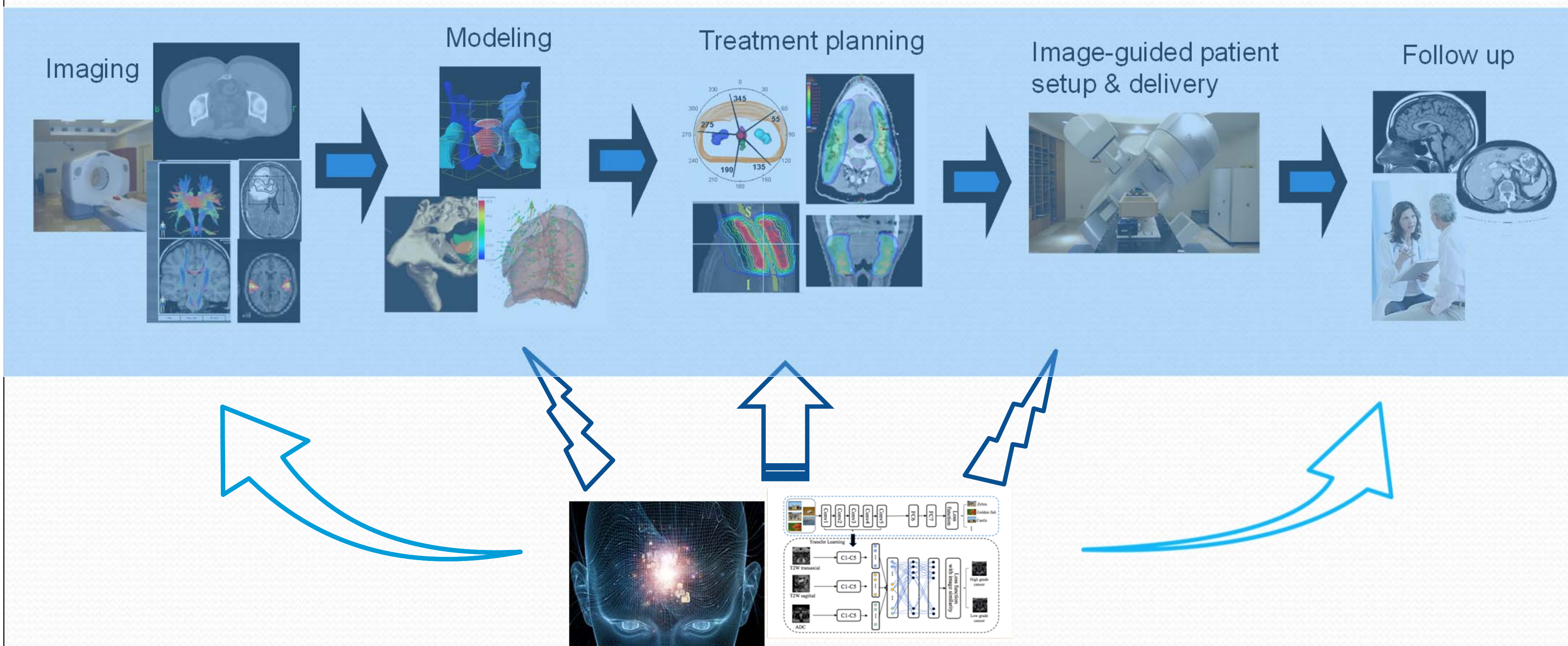
Imaging
Modeling
Treatment planning
Image-guided patient setup & delivery
Follow up

Acknowledgements

- M. Bassenne, J.-E. Bibault, Y. Chen, D. P. Capaldi, J. Fan, C. Huang, T. Islam, M. Jia, L. Shen, H. Ren, M. Ma, H. Seo, X. Li, L.Yu, T. Liu, S. Gennatas, M. Khuzani, E. Schueler, E. Simiele, K., Sivasubramanian, H. Zhang, V. Vasudevan, Y. Wu, W. Zhao, Z. Zhang, D. P.I. Capaldi

- P. Dong, B. Han, Y. Yang, N. Kovalchuk, D. Hristov, L. Skinner, C. Chuang, L. Wang, J. Lewis, D. Chang, D. Toesca, Q. Le, S. Soltys, M. Buyounouski, H. Bagshaw, S. Hancock, G. Pratx, R. Li, J. Pauly, S. Boyd, ….

- Funding: NIH/NCI/NIBIB, DOD, NSF, ACS, Varian, & Google.